CAMA

Centre for Applied Macroeconomic Analysis

Sectoral Spillovers in Inflation Dynamics: Empirical Evidence from Network Propagation

CAMA Working Paper 63/2025 November 2025

Yun Young Gwak Monash University Bank of Korea Centre for Applied Macroeconomic Analysis, ANU

Abstract

Distinguishing between sector-specific and aggregate shocks and assessing their contributions to inflation are vital for informed policy. This paper quantifies cross-sectoral spillovers in U.S. consumer price inflation using a factor-adjusted network approach that jointly models aggregate factors and sectoral network propagation. Using disaggregated personal consumption expenditure data across 26 sectors from 1959–2024, the model employs Lasso nuclear-norm regularization to estimate high-dimensional VARs while controlling for aggregate influences. Cross-sectoral spillovers account for roughly two-fifths of total price variation—more than twice the share attributable to aggregate factors—and are systematically mismeasured in conventional models: factor models understate spillovers by absorbing network transmission into common components, while VARs without factors overstate them by conflating comovement with propagation. The spillover structure is highly granular, dominated by large consumerfacing sectors such as food, furnishings, and services, with gasoline exerting more moderate but persistent effects. Spillovers propagate mainly through backward production linkages and scale with sector size, indicating that large downstream sectors play a disproportionate role in transmitting sector-specific shocks across the price network. The findings underscore the need for integrating sectoral networks and aggregate factors in modeling inflation dynamics and policy design.

Keywords

sectoral spillovers, network connectedness, inflation, cross-sectoral transmission



C32, C38, E31, E32

Address for correspondence:

(E) cama.admin@anu.edu.au

ISSN 2206-0332

<u>The Centre for Applied Macroeconomic Analysis</u> in the Crawford School of Public Policy has been established to build strong links between professional macroeconomists. It provides a forum for quality macroeconomic research and discussion of policy issues between academia, government and the private sector.

The Crawford School of Public Policy is the Australian National University's public policy school, serving and influencing Australia, Asia and the Pacific through advanced policy research, graduate and executive education, and policy impact.

Sectoral Spillovers in Inflation Dynamics: Empirical Evidence from Network Propagation

Yun Young Gwak*

Department of Economics, Monash University
Bank of Korea
Centre for Applied Macroeconomic Analysis

November 16, 2025

Abstract

Distinguishing between sector-specific and aggregate shocks and assessing their contributions to inflation are vital for informed policy. This paper quantifies cross-sectoral spillovers in U.S. consumer price inflation using a factor-adjusted network approach that jointly models aggregate factors and sectoral network propagation. Using disaggregated personal consumption expenditure data across 26 sectors from 1959–2024, the model employs Lasso nuclear-norm regularization to estimate high-dimensional VARs while controlling for aggregate influences. Cross-sectoral spillovers account for roughly two-fifths of total price variation—more than twice the share attributable to aggregate factors—and are systematically mismeasured in conventional models: factor models understate spillovers by absorbing network transmission into common components, while VARs without factors overstate them by conflating comovement with propagation. The spillover structure is highly granular, dominated by large consumer-facing sectors such as food, furnishings, and services, with gasoline exerting more moderate but persistent effects. Spillovers propagate mainly through backward production linkages and scale with sector size, indicating that large downstream sectors play a disproportionate role in transmitting sector-specific shocks across the price network. The findings underscore the need for integrating sectoral networks and aggregate factors in modeling inflation dynamics and policy design.

JEL Classification: C32, C38, E31, E32

Keywords: sectoral spillovers, network connectedness, inflation, cross-sectoral transmission

^{*}Correspondence to: Department of Economics, Monash University, 900 Dandenong Road, Caulfield East, Victoria 3145, Australia. E-mail: yunyoung.gwak@monash.edu.

1 Introduction

Inflation is often treated as a single, economy-wide phenomenon, yet sectoral price dynamics reveal substantial and persistent heterogeneity beneath the aggregate numbers. As shown in Figure A1, sectoral inflation rates frequently diverge from one another, sometimes moving together in broad alignment—as during the Great Inflation of the 1970s and the recent post-COVID surge—and at other times offsetting one another, as during the Great Moderation. These patterns highlight that aggregate inflation is not simply the outcome of uniform sectoral responses to common shocks, but the net result of diverse sectoral forces. This raises a central question for both economists and policymakers: to what extent do aggregate inflation dynamics reflect the propagation of sector-specific shocks across sectors, rather than purely economy-wide disturbances? The answer has direct policy implications. If sectoral shocks and their spillovers contribute materially to aggregate inflation, it underscores the need to monitor sector-specific disturbances and their transmission channels. Conversely, if aggregate forces dominate, sectoral dispersion is largely incidental, and stabilization policies would primarily need to address economy-wide conditions.

Recent studies using disaggregated data find that sector-specific shocks can significantly influence aggregate dynamics, challenging traditional views that such shocks average out at the macro level. Theoretical and quantitative work demonstrates this through calibrated models of production networks and sectoral heterogeneities (e.g., Gabaix 2011; Carvalho and Gabaix 2013; Acemoglu et al. 2012, 2017; Baqaee and Farhi 2019, 2020; Pasten et al. 2020; Carvalho et al. 2021; Pasten et al. 2024), while empirical investigations quantify the implied effects of these mechanisms using observed sectoral data (e.g., Li and Martin 2019; Smets et al. 2019; Ghassibe 2021; Das et al. 2022; Schneider 2023; De Graeve and Schneider 2023; Luo and Villar 2023). However, much of the literature remains theoretical, with the empirical literature often concentrating either on the direct effects of shocks or on propagation mechanisms embedded within specific structural models that impose particular functional forms for intersectoral transmission. While these approaches provide valuable discipline and testable predictions, they leave open the question of what the effective propagation structure looks like when estimated directly from the data, and how the patterns that emerge compare to theoretical benchmarks. Moreover, disentangling genuine cross-sectoral spillovers from common aggregate factors remains an empirical challenge that requires flexible, data-driven methods.

This paper revisits the question by applying econometric tools designed to capture propagation effects, providing a sharper empirical lens on the contribution of sectoral shocks and spillovers to aggregate inflation. Specifically, the analysis combines recent advances in high-dimensional VAR models with common factors with the now widely used network connectedness framework to quantify the strength and direction of inter-sectoral spillovers. Lasso nuclear-norm regularization separates aggregate dynamics, captured by dense common factors, from sector-specific interactions represented by sparse transition matrices. Within the network framework, a generalized identification strategy exploits the full covariance structure of residuals, enabling spillovers to be estimated without restrictive assumptions such as limiting them to input—output

¹Figure A1 is reported in the Online Appendix.

²This line of research builds on a long-standing literature that began with early challenges to the representative-agent paradigm—see, e.g., Long and Plosser 1983 and Horvath 1998, 2000—and continues to grow with increasingly detailed data and refined methods.

³Sectoral shocks refer to idiosyncratic disturbances specific to one or a few sectors, in contrast to aggregate shocks that affect all sectors simultaneously. Sectoral shocks inherently lead to relative price changes, whereas aggregate shocks typically drive broad movements in the general price level.

linkages. To assess the contribution of this approach, I compare the baseline specification against two nested counterfactual benchmarks: a restricted pure VAR that attributes all comovement to spillovers by shutting down the common component, and a factor model that attributes all comovement to aggregate factors by shutting down intersectoral propagation. The empirical application uses disaggregated U.S. price and consumption data for 26 final goods and 58 intermediate sectors from 1959:Q2 to 2024:Q2.

The analysis yields three main results. The central finding is that cross-sectoral spillovers contribute substantially to aggregate consumer price inflation, accounting for nearly two-fifths of total price variation—more than twice the contribution of aggregate factors. Conventional empirical frameworks yield distorted estimates: factor models systematically understate spillovers by attributing correlated movements to common shocks, while pure VARs overstate them by conflating comovement with propagation. Simulation exercises confirm that the proposed factor-adjusted network VAR recovers true propagation dynamics more accurately than either conventional benchmark. Next, the spillover structure is highly granular. A small set of large, consumer-facing sectors—particularly food, furnishings, and services—act as persistent net transmitters, while others, such as gasoline, exert more moderate but durable effects. Conventional models often misclassify these roles, either diluting or exaggerating their relative importance. Lastly, the propagation mechanism shaping consumer price inflation operates mainly through backward production linkages and scales with sectoral size. Large downstream, consumer-oriented sectors transmit price pressures upstream, showing that inflation persistence arises through the networked amplification of sector-specific demand shocks via input demand channels.

Together, these findings highlight the sensitivity of spillover estimates to modeling choices and underscore the importance of jointly accounting for both aggregate factors and sectoral networks when assessing the impact of sectoral shocks on aggregate inflation—linking this work to broader efforts to trace the microeconomic origins of macroeconomic fluctuations.

Related Literature. – This paper contributes to two central strands in the literature on the microeconomic origins of macroeconomic fluctuations, particularly focused on studying inflation dynamics. The first concerns aggregation, building on seminal works such as Boivin et al. (2009), Reis and Watson (2010), Ahn and Luciani (2025), and Schneider (2023), who use factor-analytic methods to decompose the relative contributions of aggregate and sectoral shocks to inflation variation. These approaches provide valuable insights into the importance of sectoral heterogeneity, though they typically abstract from modeling the cross-sectoral dynamics through which shocks propagate. This paper complements this literature by embedding factor structures within a VAR framework that explicitly captures sectoral propagation dynamics, allowing for a joint assessment of both common aggregate forces and the network of sectoral spillovers.

The second strand relates to sectoral propagation and network effects. A substantial theoretical and quantitative literature demonstrates how sectoral heterogeneity and production networks amplify idiosyncratic shocks into aggregate fluctuations (Carvalho et al., 2021; Pasten et al., 2020, 2024). Empirical investigations have documented these propagation effects in the context of prices: Smets et al. (2019) examine pipeline pressures in sectoral inflation, Luo and Villar (2023) trace shock propagation through input-output linkages to prices, Ghassibe (2021) quantifies network contributions to monetary policy transmission to consumption and prices, and Mlikota (2025) analyzes forecasting performance in Network-VAR models

⁴There is also an empirical literature that applies factor-analytic decompositions to sectoral output dynamics, including Foerster et al. (2011), Li and Martin (2019), and De Graeve and Schneider (2023).

with lagged production linkages. These studies highlight the importance of propagation, typically by embedding specific structural assumptions about the transmission channels. This paper contributes to this strand of the literature by estimating the effective propagation structure directly from the data, providing a complementary perspective that reveals which sectoral connections emerge as empirically significant and how the estimated patterns compare to conventional benchmarks. The results further illustrate why Hulten (1978)'s theorem⁵ does not hold in the presence of economic frictions, as shock propagation reflects the interplay of production linkages, various frictions, and sectoral heterogeneities.

Methodologically, this paper contributes to the expanding network connectedness literature initiated by Diebold and Yilmaz (2009, 2012), which has been extensively applied in finance and energy markets but rarely to sectoral prices and inflation. Leveraging recent advances that integrate lasso and nuclear norm regularization for handling high-dimensional data with factor structures (Demirer et al., 2018; Barigozzi and Brownlees, 2019; Miao et al., 2023; Barigozzi et al., 2024), this study builds on the estimation procedure of Miao et al. (2023) to improve inference on sectoral spillovers. Unlike Demirer et al. (2018), who impose sparsity without factors, or Barigozzi et al. (2024), who apply sparsity only to idiosyncratic VAR components, this model enforces sparsity across the entire system, consistent with theory predicting that sectoral propagation amplifies both sectoral and aggregate shocks (Ghassibe, 2021).

In relation to these literatures, this study is most closely related to Schneider (2023) and Furkan et al. (2025), who also analyze sectoral inflation dynamics, though it differs by being more data-driven and agnostic about propagation structure. Schneider (2023) uses a factor-augmented VAR to decompose aggregate and sectoral shocks but abstracts from modeling cross-sectoral spillovers; this paper advances the methodology by explicitly capturing spillover dynamics alongside factor structures. Furkan et al. (2025) also examines sectoral inflation but differs in two key ways: they apply pilot OLS with nuclear norm penalization following Moon and Weidner (2023) and restrict network links to the input—output matrix. In contrast, this study employs lasso—nuclear-norm estimation based on Miao et al. (2023) to freely estimate the full transition matrices without imposing a priori structural constraints on which sectoral connections matter.

The remainder of the paper is organized as follows: Section 2 introduces the factor-adjusted network approach. Section 3 presents empirical evidence quantifying cross-sectoral spillovers. Section 4 further examines the implications of sectoral propagation dynamics on granularity. Section 5 tests theoretical mechanisms through dyadic regressions. Section 6 provides robustness checks, and Section 7 concludes.

2 Factor-Adjusted Network Approach

This section outlines the factor-adjusted network approach central to the paper's methodology, which jointly captures aggregate dynamics and sectoral propagation while avoiding the systematic biases of conventional approaches. Section 2.1 describes the high-dimensional VAR model with common factors, nesting two benchmark specifications. Section 2.2 details the estimation approach using lasso-nuclear norm regularization. Section 2.3 introduces the connectedness measures used to quantify spillovers.

⁵"The Hulten theorem states that for efficient economies and under minimal assumptions, the impact on aggregate TFP of a microeconomic TFP shock is equal to the shocked producer's sales as a share of GDP." (Baqaee and Farhi, 2019)

2.1 High-dimensional VAR with common factors

This paper specifies a high-dimensional vector autoregression (VAR) of order p for an N-dimensional time series that incorporates common factors as follows:

$$Y_{t} = \sum_{k=1}^{p} B_{k} Y_{t-k} + \Lambda F_{t} + u_{t}, \quad t = 1, \dots, T,$$
(1)

where $Y_t = (y_{1t}, \dots, y_{Nt})'$ is the vector of observed variables, B_k are $N \times N$ transition matrices, Λ is an $N \times R$ matrix of factor loadings, F_t is an R-dimensional vector of common factors, and u_t is an N-dimensional vector of idiosyncratic errors. For compactness, the system in Equation (1) can be rewritten as:

$$\underbrace{\begin{bmatrix} Y_1' \\ \vdots \\ Y_T' \end{bmatrix}}_{\mathbf{Y}} = \underbrace{\begin{bmatrix} Y_0' & \cdots & Y_{1-p}' \\ \vdots & \ddots & \vdots \\ Y_{T-1}' & \cdots & Y_{T-p}' \end{bmatrix}}_{\mathbf{Y}} \underbrace{\begin{bmatrix} B_1' \\ \vdots \\ B_p' \end{bmatrix}}_{\mathbf{R}} + \underbrace{\begin{bmatrix} F_1' \\ \vdots \\ F_T' \end{bmatrix}}_{\mathbf{F}} \underbrace{\begin{bmatrix} \lambda_1' \\ \vdots \\ \lambda_N' \end{bmatrix}}_{\mathbf{N}'} + \underbrace{\begin{bmatrix} u_1' \\ \vdots \\ u_T' \end{bmatrix}}_{\mathbf{U}} \tag{2}$$

The model relaxes Gaussian assumptions by allowing weak cross-correlation in idiosyncratic errors, while factors follow a stationary linear process with potentially nonzero mean and remain mutually orthogonal. Both factors and errors may exhibit serial correlation, modeled as:

$$F_t = \phi^f F_{t-1} + \epsilon_t^f, \quad u_t = \phi^u u_{t-1} + \epsilon_t^u.$$
 (3)

While joint estimation is theoretically feasible, this study employs the two-step estimation procedure of Bernanke et al. (2005) for computational tractability. Importantly, Bernanke et al. (2005) show that this two-step approach closely approximates full joint estimation results.

Data Description and Lag Selection. – The empirical application considers N = 52 series consisting of quarterly U.S. BEA PCE price indices and real consumption expenditure indices across 26 sectoral categories, spanning 1959 Q1 to 2024 Q2. The sectors are disaggregated to the third or fourth tier based on similar degrees of nominal rigidity following Carvalho et al. (2021). The series for each of the sectors are transformed into annualized quarterly growth rates by taking first differences of logarithms to achieve stationarity and standardized locally to zero mean and unit variance for factor estimation.

The lag length for the VAR model is set to p = 1, based on the growth ratio criterion introduced by Miao et al. (2023), which consistently selects the optimal lag order in high-dimensional settings.

Nested Models for Comparison. – One of the key advantages of this model is that it captures both the dynamic structure of the data through the lagged term \mathbf{XB}' and the strong cross-sectional interactions via

⁶For the full list and summary statistics, see Appendix B. Following Carvalho et al. (2021), I start with 27 sectoral categories, excluding the low-share category for non-profit institutions serving households (NPISHs) to align with household consumption theory. Compared to Carvalho et al. (2021), I further exclude one full category—used motor vehicles (1%)—and one subcategory—recreational books (0.1–0.2%)—due to inconsistencies with input–output and micro price rigidities data from Pasten et al. (2020), resulting in a total of 26 sectors included. The remaining sectors account for 96.38% of the total share.

⁷The local detrending method uses Tukey's biweight function with a bandwidth of 100 quarters (25 years); see Tukey (1960).

the common component $F\Lambda'$. In this regard, it nests two familiar benchmark specifications:

$$Y = \begin{cases} XB' + U, & \text{if } F\Lambda' = 0 \\ F\Lambda' + U, & \text{if } XB' = 0 \end{cases} \text{ (Restricted Model 1: Pure VAR),}$$

$$(4)$$

where the factor model specification (DFM) arises when the lagged term is restricted to zero (XB' = 0), 8 and the pure VAR without factors (PVAR) arises when the common component is excluded (FA' = 0). I adopt the labels PVAR and DFM for expositional clarity, while acknowledging that their usage varies across the literature. This nesting illustrates the model's ability to unify factor-based and purely dynamic VAR approaches within a single framework.

2.2 Estimation: ℓ_1 -nuclear-norm regularization

Estimating a high-dimensional factor-adjusted VAR model presents two main challenges. First, the dimensionality of the data relative to the sample size creates a degrees-of-freedom problem, especially when including multiple sectoral variables and their lags. Second, the presence of lagged terms means that applying principal component analysis directly to the data matrix does not yield consistent estimates of the common factors.

To overcome these challenges, this study employs an ℓ_1 -nuclear-norm regularization approach. The ℓ_1 -norm (Lasso) induces sparsity in the transition matrices, distinguishing them from the dense factor structure, while the nuclear norm penalty encourages the common component to be low-rank. This approach balances the need to reduce overfitting and the curse of dimensionality while capturing common aggregate effects through factors. For the nonzero coefficients identified by Lasso, the estimates are asymptotically equivalent to oracle least squares estimates, providing strong theoretical support for the sparsity assumption.

While sparse modeling may not suit all macroeconomic datasets (Giannone et al., 2021), the focus on disaggregated sectoral data supports combining a sparse VAR structure with a dense factor model. By accounting for dominant cross-sectional dependence through factors, the remaining residual dependence is expected to be weak, making the sparse VAR assumption reasonable.⁹

Following Miao et al. (2023), estimation proceeds in three steps to jointly estimate the transition matrix B, the factors F, and the loadings Λ . The first step solves the following penalized least squares problem:

$$\underset{B,\Theta}{\arg\min} \; \frac{1}{2NT} \| Y - XB - \Theta \|_F^2 + \gamma_1 \frac{1}{N} \| B \|_1 + \gamma_2 \frac{1}{NT} \| \Theta \|_* \quad \text{(First Step)} \tag{5}$$

where Y is the observed data, X the lagged regressors, Θ the common component, $\|\cdot\|_F$ the Frobenius norm, $\|\cdot\|_1$ the lasso norm, and $\|\cdot\|_*$ the nuclear norm. The tuning parameters γ_1 and γ_2 control the penalties. Applying singular value decomposition to Θ yields initial estimates of the factors F.

In the second step, the model updates estimates of B and Λ by regressing Y on X and the estimated

⁸Alternatively, this specification may be referred to as a dynamic factor model, following Stock and Watson (2016), to distinguish it from factor-augmented vector autoregressions that incorporate observable factors.

⁹The sparsity in the transition matrix reflects a sparse Granger-causality structure, without ruling out indirect network effects (Barigozzi and Brownlees, 2019; Barigozzi et al., 2024).

factors, applying a plain lasso penalty to B:

$$\underset{B,\Lambda}{\operatorname{arg\,min}} \ \frac{1}{2T} \|Y - XB - F\Lambda'\|_F^2 + \gamma_3 \|B\|_1 \quad \text{(Second Step)}$$

The third step refines these estimates via an iterative conservative lasso that adaptively reweights the penalty on *B* to revisit variables excluded by earlier steps:

$$\underset{B^{(l)},\Lambda}{\arg\min} \ \frac{1}{2T} \|Y - XB^{(l)} - F^{(l-1)}\Lambda'\|_F^2 + \gamma_4 \sum_k w_k^{(l)} |B_k^{(l)}| \quad \text{(Third Step)}$$

where the weights $w_k^{(l)}$ are set as

$$w_k^{(l)} = \begin{cases} 1, & \text{if } |B_k^{(l-1)}| < \alpha \gamma_4, \alpha > 0 \\ 0, & \text{otherwise} \end{cases}$$

This weighting downweights large coefficients, allowing recovery of important variables missed initially. Factors $F^{(l)}$ are updated via singular value decomposition at each iteration.

Tuning Parameters. – The tuning parameters for the ℓ_1 penalties on the transition matrices in the second and third steps are selected via five-fold stratified cross-validation combined with stable selection procedures. Building on Miao et al. (2023), this paper implements two key extensions. First, stratified cross-validation is performed using K-means clustering¹⁰ on the standardized total sum of absolute deviations from the local trend, ensuring training and testing sets maintain similar distributions of stable and unstable periods (Kohavi, 1995). Second, to mitigate further potential LASSO instability I apply stability selection: over 50 random cross-validation partitions I record each coefficient's selection frequency (for given α), retain coefficients selected in ≥ 60% of runs¹¹, and refit the model on this restricted set.

Number of factors. – Finally, unlike the original approach that selects the number of factors solely via singular value thresholding, this study determines the number of aggregate factors by combining data-driven criteria with macroeconomic knowledge. For a detailed discussion, see Appendix C.

2.3 Variance Decomposition and Connectedness Approach

dations from Meinshausen and Bühlmann (2010).

To analyze how shocks propagate across sectors, it is crucial to separate the contributions of common (aggregate) shocks from idiosyncratic (sector-specific) shocks to the variation in sectoral prices. Using the estimated factor-adjusted VAR model, this analysis performs a variance decomposition that partitions total variation into components driven by each shock type, thus isolating the idiosyncratic dynamics for the subsequent connectedness analysis.

Common versus idiosyncratic shares of variance. – The N-dimensional VAR(p) can be rewritten as an

¹⁰Starting with K = 8 clusters, those with fewer than 5 observations are merged into the nearest cluster, yielding 6–8 clusters. ¹¹This procedure enhances robustness by focusing on consistently selected predictors. The 60% threshold aligns with recommen-

Np-dimensional VAR(1):

$$\begin{bmatrix}
Y_{t} \\
Y_{t-1} \\
Y_{t-2} \\
\vdots \\
Y_{t-p+1}
\end{bmatrix} =
\begin{bmatrix}
B_{1} & B_{2} & \cdots & B_{p-1} & B_{p} \\
I_{N} & 0 & \cdots & 0 & 0 \\
0 & I_{N} & \cdots & 0 & 0 \\
\vdots & \vdots & \ddots & \vdots & \vdots \\
0 & 0 & \cdots & I_{N} & 0
\end{bmatrix}
\begin{bmatrix}
Y_{t-1} \\
Y_{t-2} \\
Y_{t-3} \\
\vdots \\
Y_{t-p}
\end{bmatrix} +
\begin{bmatrix}
\Lambda F_{t} \\
0 \\
0 \\
\vdots \\
0
\end{bmatrix} +
\begin{bmatrix}
u_{t} \\
0 \\
0 \\
\vdots \\
0
\end{bmatrix}.$$
(8)

Expressing the process in its Wold representation,

$$X_{t+1} = \sum_{j=0}^{\infty} \Phi_j(\mathscr{F}_{t-j} + \mathscr{U}_{t-j}) = X_{t+1}^{(f)} + X_{t+1}^{(u)}, \tag{9}$$

where $X_{t+1}^{(f)}$ and $X_{t+1}^{(u)}$ correspond to components driven by common factors and idiosyncratic shocks, respectively. Focusing on the *i*-th entry of X_{t+1} , denoted y_{it} , the decomposition can be written as

$$y_{it} = y_{it}^{(f)} + y_{it}^{(u)}, (10)$$

with

$$y_{it}^{(f)} = \sum_{j=0}^{\infty} (e_{1,p} \otimes e_{i,N})' \Phi_j(e_{1,p} \otimes \Lambda) F_{t-j} = \sum_{j=0}^{\infty} \alpha_{iN}^{(f)}(j) F_{t-j},$$

$$y_{it}^{(u)} = \sum_{j=0}^{\infty} (e_{1,p} \otimes e_{i,N})' \Phi_j(e_{1,p} \otimes I_N) u_{t-j} = \sum_{j=0}^{\infty} \alpha_{iN}^{(u)}(j) u_{t-j},$$

where $e_{m,n}$ is the m-th column of the identity matrix I_n , and \otimes denotes the right-hand Kronecker product. Here, $y_{it}^{(f)}$ captures the variation explained by the factors, while $y_{it}^{(u)}$ isolates the idiosyncratic component.

The shares of variance explained by each component are obtained by comparing the variance contributions across all *N* variables:

$$\frac{\sum_{i=1}^{N} \text{var}(y_{it}^{(f)})}{\sum_{i=1}^{N} \text{var}(y_{it})} \quad \text{and} \quad \frac{\sum_{i=1}^{N} \text{var}(y_{it}^{(u)})}{\sum_{i=1}^{N} \text{var}(y_{it})}.$$

The resulting variance shares rest on the orthogonality between the common factors and the idiosyncratic error terms. ¹² These shares are computed cumulatively over the sample and provide a data-driven decomposition of aggregate and individual dynamics. By isolating the idiosyncratic variation from the common factor structure, this approach enables a clearer interpretation of sector-specific behavior, which are often correlated. This distinction is essential for the subsequent network connectedness analysis, which focuses exclusively on the propagation of sectoral shocks.

Network connectedness. – Building on the idiosyncratic components isolated above, this analysis applies the Diebold–Yilmaz network connectedness framework (Diebold and Yilmaz, 2009, 2012, 2014, 2023) to quantify spillovers across sectors arising from idiosyncratic shocks. The framework constructs an $N \times N$ connectedness matrix C^H based on the H-step-ahead generalized impulse response functions (Koop et al.,

¹²This approach treats the common factors and idiosyncratic components as impulses with one-standard-deviation innovations.

1996; Pesaran and Shin, 1998), which identify shock responses accounting for correlations among residuals by using the full covariance matrix, thus avoiding variable ordering assumptions. In the resulting forecast error variance decomposition of the VAR residuals, each element C_{ij}^H measures the fraction of sector i's forecast error variance attributable to shocks originating in sector j. Formally,

$$C_{ij}^{H} = \frac{d_{ij}^{H}}{\sum_{k=1}^{N} d_{ik}^{H}}, \quad \text{where} \quad d_{ij}^{H} = \frac{\sigma_{jj}^{-1} \sum_{h=0}^{H-1} \left(\alpha_{iN}^{(u)}(h) \Sigma_{u} e_{j,N}\right)^{2}}{\sum_{h=0}^{H-1} \alpha_{iN}^{(u)}(h) \Sigma_{u} \alpha_{iN}^{(u)}(h)'}.$$
(11)

Here, σ_{jj} is the standard deviation of variable j, $\alpha_{iN}^{(u)}(h)$ are the generalized impulse response coefficients from the idiosyncratic component, Σ_u is the covariance matrix of the idiosyncratic residuals, and $e_{j,N}$ is the j-th column of the identity matrix.

Initially, the connectedness analysis produces a 52×52 matrix, with columns representing shocks from 26 sectoral prices and 26 sectoral consumptions, and rows representing responses in the same variables. Each row sums to 100%, reflecting shares of the idiosyncratic variation only. To focus on sector-by-sector relationships, the corresponding price and consumption shock columns for each sector are summed, resulting in a 52×26 matrix. This matrix is then partitioned into two 26×26 blocks: the upper block captures sectoral price responses, and the lower block captures sectoral consumption responses. Finally, to interpret each element as a share of the total variation, the rows are rescaled by the sector's idiosyncratic variance share obtained from the variance decomposition.

In the final step, the connectedness matrix's pairwise directional spillovers—from column sector j to row sector i, represented by each element—are aggregated into summary measures:

- "TO" = $C_{\bullet \leftarrow j}^H = \sum_{i \neq j} C_{ij}^H$, total spillovers transmitted by sector j;
- 'FROM' = $C_{i \leftarrow \bullet}^H = \sum_{j \neq i} C_{ij}^H$, total spillovers received by sector i;
- 'NET' = TO FROM, indicating the net sectoral influence in the network¹³;
- 'TCI' (Total Connectedness Index), system-wide connectedness:

$$TCI = \frac{1}{N} \sum_{i,j;j \neq j} C_{ij}^H. \tag{12}$$

Together, these connectedness measures provide a comprehensive quantification of sectoral shock propagation within the broader system, with rescaling ensuring their interpretation relative to total variation.

Having established the methodological framework, the analysis now turns to the empirical results. The following sections apply the baseline model to U.S. sectoral price and consumption data to quantify the magnitude of cross-sectoral spillovers in inflation, examine their sectoral distribution, and assess how these patterns compare across different model specifications.

¹³For policy analysis and network visualization, TO indices are weighted by sectoral consumption shares to reflect macroeconomic importance, while NET indices remain unweighted to capture pure directional spillover asymmetries. Conceptually, TO, FROM, and NET correspond closely to out-degree, in-degree, and degree centrality in network science (see Newman 2010). The key distinction is that, in the Diebold–Yilmaz framework, edges are horizon-specific and weighted by forecast error variance shares. In macro-financial applications, empirical analysis typically focuses on horizons at which the variance decomposition has stabilized, thereby capturing the persistent spillover structure rather than short-run transients.

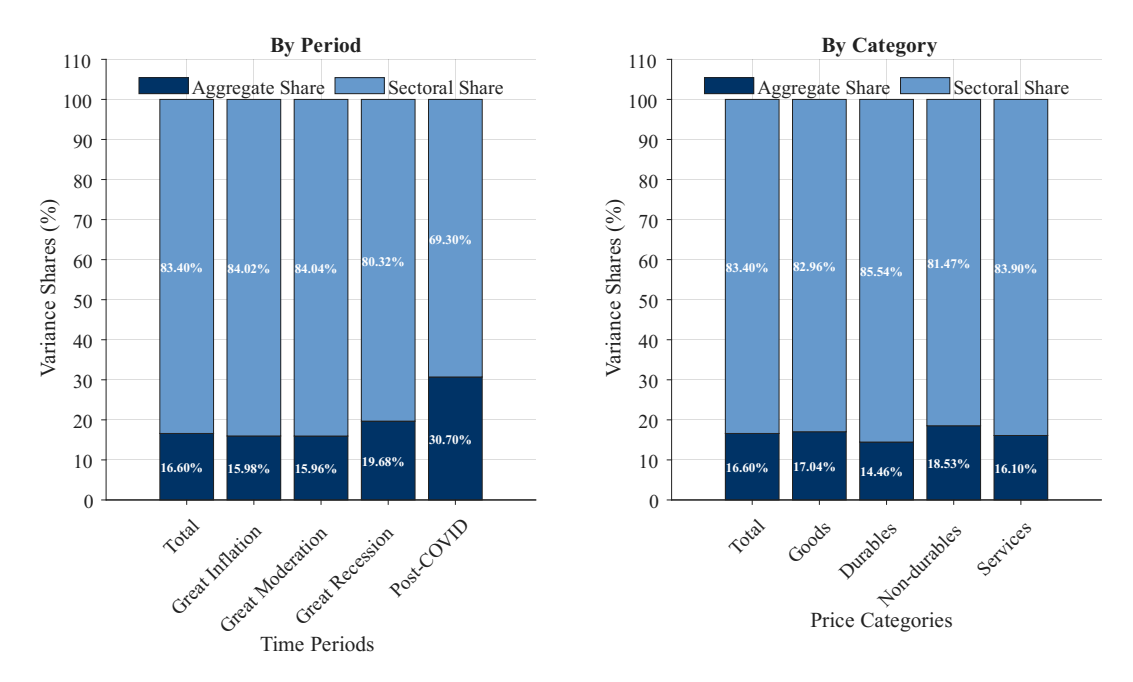


Figure 1: Baseline Model Variance Decomposition by Period and Category

Notes: (a) This figure shows the variance decomposition for the baseline model across time periods (left panel) and sectoral categories (right panel). Stacked bars represent aggregate share (dark blue, bottom) and sectoral share (medium blue, top) that sum to 100%. (b) Numbers inside bars indicate precise percentage values to two decimal places.

3 Magnitude of Cross-Sectoral Spillovers

This section presents baseline evidence of cross-sectoral spillovers using a model that incorporates both common factors and lagged cross-sectoral dynamics. Section 3.1 first isolates the contributions of aggregate shocks and section 3.2 then measures the magnitude cross-sectoral spillovers from sectoral shocks.

3.1 Variance Decomposition Between Aggregate and Sectoral Shocks

To control for the effects of aggregate shocks, the analysis begins by assessing the relative aggregated contributions of sectoral versus aggregate shocks to price variation. The factor selection (detailed in Appendix C) identifies three common factors that capture aggregate dynamics while allowing the baseline model to isolate cross-sectoral spillovers.

Figure 1 presents the baseline model's variance decomposition, revealing the predominant role of sectoral shocks in driving price dynamics with important temporal and cross-sectoral heterogeneity. The results show that sectoral shocks explain approximately 83% of the total variation in prices, while aggregate shocks account for about 17%. This relatively low share of aggregate variation aligns with prior findings indicating that aggregate factors typically explain a modest portion of inflation variability at disaggregated levels. For example, Boivin et al. (2009) report aggregate factors explaining roughly 15–17% of monthly inflation variance, with lower shares reflecting higher-frequency noise.

The dominance of sectoral shocks is expected given the heterogeneous nature of sectoral pricing, which arises from diverse input-output linkages, idiosyncratic demand and supply conditions, and varying price rigidities. Aggregate shocks capture broad economy-wide trends but fail to account for the rich cross-sectoral

heterogeneity driving most price variation. This finding reinforces the importance of explicitly modeling sectoral-level shocks to understand the full dynamics of price fluctuations.

The left panel demonstrates that sectoral shocks consistently dominate across all time periods, explaining between 69% (Post-COVID) and 84% (Great Moderation) of price variance. This temporal variation reflects the varying intensity of aggregate disturbances across economic episodes: periods of heightened macroeconomic volatility naturally exhibit larger aggregate factor contributions, while periods of relative stability see sectoral forces dominate more completely. These results are consistent with prior research reporting lower aggregate shares during the Great Moderation (Foerster et al., 2011), and higher shares during the Great Recession (Li and Martin, 2019).

The right panel reveals systematic differences across product categories that align with economic intuition about sectoral characteristics. Services exhibit higher sectoral share (84%) than goods (83%), consistent with their more localized and less tradable character, which increases the relative importance of sector-specific dynamics. Within goods, durables show higher sectoral shares (86%) than non-durables (81%), reflecting the more heterogeneous and cyclically sensitive nature of durable goods markets where idiosyncratic factors like product differentiation and replacement cycles play larger roles.

Model Comparison. – To benchmark the baseline specification, I consider two restricted alternatives designed to disentangle the contributions of cross-sectoral dynamics and latent common factors. In the first, I impose a zero restriction on the dynamic sectoral transmission matrix (B = 0), thereby eliminating a common intersectoral propagation channel and attributing all co-movement to common factors. In the second, I set the factor loadings to zero ($\Lambda = 0$), yielding a pure VAR in sectoral variables without latent components, such that all co-movement arises from direct sectoral interactions. These restricted specifications provide informative benchmarks for assessing the relative importance of dynamic transmission channels and common factors in shaping measured spillovers.

Figure D1 summarizes variance decompositions across the three specifications. The baseline model lies consistently between the benchmarks, with aggregate shares ranging from 17% during the Great Moderation to 31% in the post-COVID period. Among these, the factor model specification (DFM) is especially relevant, as it represents the conventional model widely used to distinguish sectoral from aggregate dynamics. Consistent with a recurring theme in this paper, however, it systematically overstates aggregate contributions—by 10–15 percentage points relative to the baseline—because cross-sectoral spillovers are absorbed into its factors, thereby inflating the apparent role of aggregate forces. This bias is particularly pronounced in services and durables, where strong sectoral propagation is misclassified as aggregate, in contrast to the baseline which identifies them as more sectoral in nature.

Conversely, the naive pure VAR (PVAR), employed in the broader network literature, attributes nearly all variation to sectoral dynamics by construction, eliminating the possibility of distinguishing genuine aggregate influences. While this specification offers a useful counterfactual for gauging the contribution of common factors, it is not a realistic representation of economic dynamics in which both aggregate and sectoral forces interact. Assuming the baseline model approximates the data-generating process, aggregate shocks explain roughly 17% of variation, but their influence can be overstated when sectoral propagation effects are improperly absorbed into common factors.

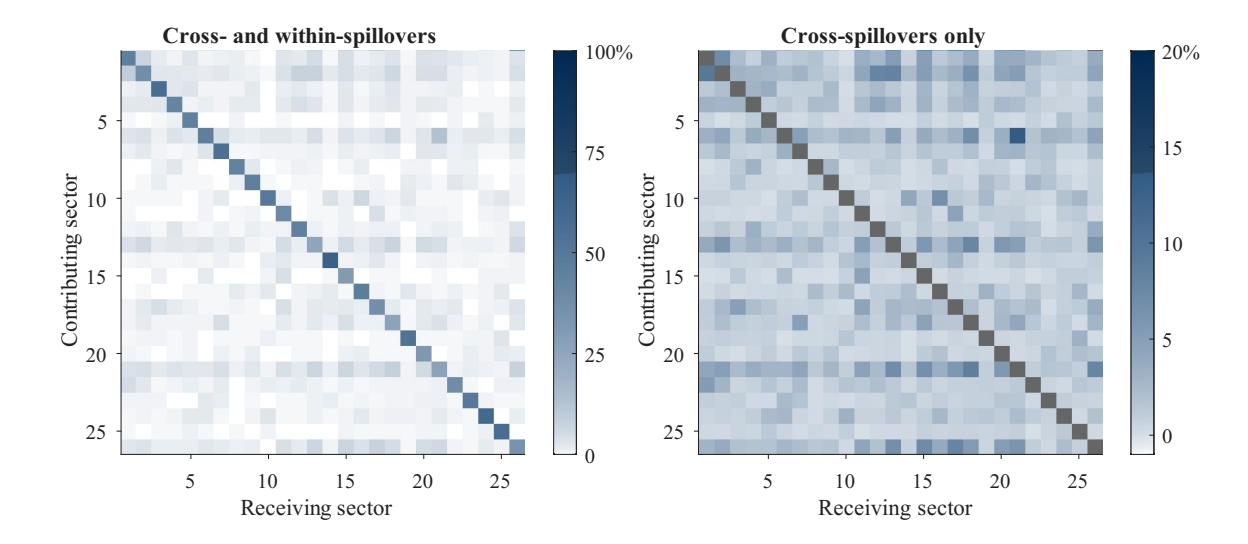


Figure 2: Baseline Model Spillover Network

Notes: (a) This figure displays connectedness matrices from the baseline model with factor structure and cross-sectoral dynamics. (b) The left panel shows the complete spillover network including within-sector effects (diagonals), scaled 0-100%. The right panel isolates cross-sectoral spillovers by masking diagonal elements, scaled 0-20% for enhanced visibility of off-diagonal patterns. (c) Darker blue shades indicate stronger spillover contributions from contributing sectors (y-axis) to receiving sectors (x-axis). (d) Matrices are based on generalized forecast error variance decompositions of the idiosyncratic component at 16 quarter horizons after controlling for the factors.

3.2 System-Wide Total Connectedness:

Next, I narrow the focus on the baseline model's spillover structure to establish the empirical foundation for cross-sectoral transmission mechanisms. The economic intuition underlying this approach rests on the recognition that modern economies are characterized by complex production networks, supply chain linkages, and demand complementarities that create systematic channels for sectoral shock transmission beyond the role of aggregate factors.

Figure 2 presents the connectedness matrix estimated from the baseline model, revealing the comprehensive network of spillover relationships across 26 sectors. In the left panel, the concentration along the diagonal confirms that sectors primarily influence themselves, consistent with theoretical expectations that own-sector effects dominate. However, the right panel, which masks diagonal elements and rescales to 0-20%, exposes extensive off-diagonal spillovers that would be overlooked in conventional analyses focused solely on aggregate dynamics. These cross-sectoral effects represent systematic transmission channels through which sectoral shocks propagate beyond their originating sectors.

In numbers, the total connectedness index (TCI) from the baseline model reaches 47.6%, indicating that almost half of idiosyncratic price movements stem from cross-sectoral spillovers rather than purely sector-specific shocks. In terms of total variation, this amounts to 39.9% of sectoral price variation. Compared to the 16.6% contribution of aggregate factors, this suggests sectoral spillovers constitute an important transmission mechanism for understanding price dynamics. This finding indicates that sectoral spillovers represent a quantitatively important component of price variation that warrants consideration alongside aggregate factors in macroeconomic models.

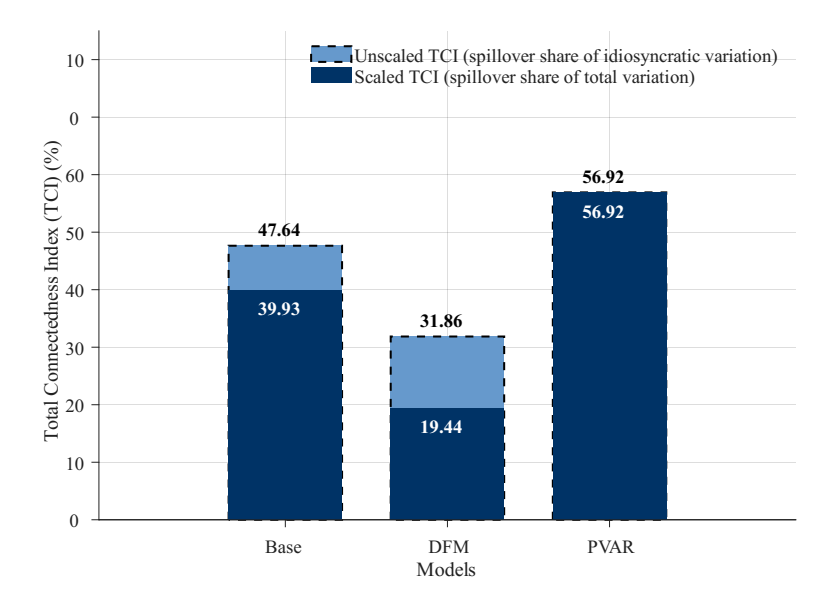


Figure 3: Total Connectedness Index Comparison Across Models

Notes: (a) This figure compares the Total Connectedness Index (TCI) across three model specifications. The TCI measures the share of forecast error variance due to cross-sectoral spillovers within the idiosyncratic component after controlling for common factors. (b) Dark blue bars show scaled TCI (spillover share of total variation), while medium blue bars with dashed borders show unscaled TCI (spillover share of idiosyncratic variation). (c) Numbers on bars indicate precise TCI values to two decimal places.

The role of cross-sectoral spillovers aligns with growing evidence on the quantitative importance of network effects for macroeconomic fluctuations. For instance, Das et al. (2022) find that spillovers from sectoral shocks are almost twice as large as own effects, while Ghassibe (2021) estimate that network channels account for 30–50% of monetary policy transmission. The results in this paper are broadly consistent with these findings: variance decompositions show comparable magnitudes of own and spillover effects that remain persistent after extensive lags, and a similar impulse response analysis indicates amplification of aggregate and sectoral shocks by 64.1% and 82.5%, respectively.

Model Comparison. – Figure 3 provides a systematic comparison of TCI estimates across the three model specifications, revealing the quantitative importance of methodological choices for spillover measurement. The baseline model's scaled TCI of 39.9% represents a middle ground between the estimates produced by restricted specifications, attributing 39.9% of total price variation to cross-sectoral spillovers from sectoral shocks.

From a theoretical perspective, this dominance of spillovers over aggregate factors reflects the increasing complexity and interconnectedness of modern production networks. The 39.9% spillover share represents the cumulative effect of numerous micro-level transmission channels: supply chain disruptions that propagate across vertically linked sectors, demand spillovers between complementary goods, and strategic pricing responses to competitors' price changes. These micro-foundations aggregate to create macro-level patterns that are as influential as traditional aggregate shocks.

In contrast, the factor model (DFM) underestimates spillovers, attributing only 19.4% of total price variation. This underestimation reflects two limitations: first, the DFM specification inflates the role of aggregate factors themselves by absorbing some spillover effects into the factor estimates and thereby compressing

the idiosyncratic share; second, it imposes independence between factor-driven and idiosyncratic dynamics, yielding an artificially sparse representation of cross-sectoral interactions, even though—as emphasized by Pasten et al. (2024) for sectoral shocks and by Ghassibe (2021) for aggregate shocks—sectoral linkages propagate and amplify disturbances of both types.

Conversely, the pure VAR (PVAR) overstates spillovers, at 56.9% compared with the baseline estimate of 39.9%. Because this specification cannot disentangle aggregate influences from genuine propagation channels, it attributes common shocks to the transition matrix, thereby exaggerating cross-sectoral effects. Together, these contrasts highlight the importance of incorporating both factor dynamics and transition linkages to recover spillovers accurately.

Overall, the variance decomposition results show that sectoral shocks explain more than 80% of price variation, with sizeable cross-sectoral spillovers representing a quantitatively important transmission mechanism. These findings emerge from the baseline model that jointly captures both aggregate factors and sectoral propagation dynamics.

3.3 Model Comparison of Sectoral Spillover Networks

Having shown that overall TCI estimates vary across model specifications, this subsection further demonstrates the value of the baseline approach by comparing sector-level spillover estimates across alternative models, illustrating how conventional frameworks can systematically bias spillover measurement.

Figure 4 compares the detailed spillover estimates across the three specifications: the restricted pure VAR without factors, the baseline model with both factors and cross-sectoral dynamics, and the factor model. As with the TCI bar plots, the heatmaps confirm systematic differences: the PVAR model (left column) overestimates spillovers, with darker shades indicating stronger connectedness, while the DFM (right column) underestimates them, with lighter shades indicating weaker connectedness. The baseline (center column) provides intermediate estimates, producing a TCI of 39.9% (as reported in the previous section), and captures spillovers while properly accounting for aggregate factors.

To better understand these differences, Figure 5 highlights the sectoral-level disparities between the baseline model and the two benchmark approaches. Sectors are sorted by their baseline TO indices (highest transmitters first) to highlight where modeling choices matter most economically. The strongest spillover transmitters in the baseline model include food services (90.6 TO index), furnishings (86.3), food (85.4), personal care (78.1), and other services (75.3), as detailed in Table C5. The difference matrices reveal systematic patterns in model disagreement that have important economic interpretations.

The left panel shows that the baseline model generally estimates lower spillovers than the PVAR, highlighted in mostly red shades, particularly for the strongest transmitting sectors (top rows), where the PVAR's inability to control for aggregate factors leads to overestimation. This pattern is economically intuitive: sectors that appear to be strong spillover transmitters in a PVAR model may actually be responding to common aggregate factors rather than genuinely transmitting idiosyncratic shocks to other sectors.

 $^{^{14}}$ Sectors are ordered by size-weighted TO indices (descending) from the baseline model, where each sector's TO index is multiplied by its consumption expenditure share. This weighting reflects economic importance: spillovers from larger sectors have greater aggregate impact than those from smaller sectors. The ΔTO bars similarly show changes in weighted TO indices across model specifications. However, individual heatmap cells remain unweighted, preserving the symmetric dyadic interpretation where cell (i,j) represents the percentage of sector j's forecast-error variance explained by shocks from sector i, regardless of sectoral size. This design choice maintains the property that TO = FROM for the system as a whole while allowing economically-weighted rankings.

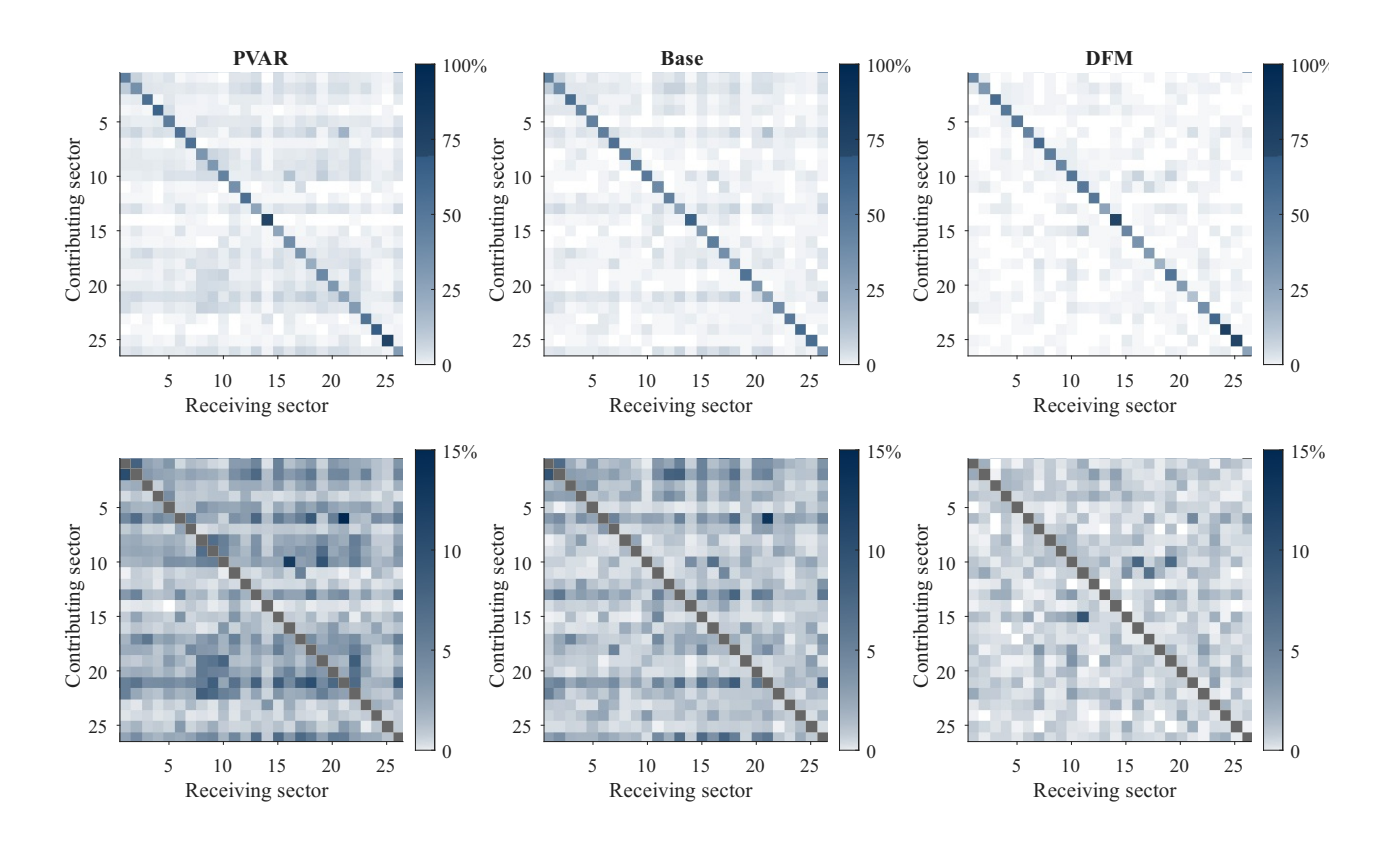


Figure 4: Cross-Model Comparison of Sectoral Spillover Networks

Notes: (a) This figure compares spillover estimates based on generalized forecast error variance decompositions over 16-quarter-horizon across three model specifications for sectoral prices. Top row shows complete connectedness matrices (0-100% scale) including within-sector effects. Bottom row isolates cross-sectoral spillovers by masking diagonal elements (0-20% scale). (b) Left column: PVAR model without factor structure. Center column: Baseline model with both factor structure (ΛF_t) and cross-sectoral dynamics (B). Right column: DFM model (B = 0) with factors but independent idiosyncratic components. (c) Darker blue indicates stronger spillovers from contributing sectors (y-axis) to receiving sectors (x-axis). Matrices are transposed so contributing sectors appear on the vertical axis.

The right panel demonstrates the opposite pattern relative to the DFM: the baseline model estimates consistently higher spillovers, indicated by mostly blue shades, especially for sectors with strong transmission roles. The ΔTO bars quantify these differences at the sectoral level, showing that modeling choices have the largest impact on sectors that serve as key nodes in the spillover network. For instance, food services shows different transmission estimates across models (90.6 in baseline vs. 16.2 in DFM), while personal care exhibits variation (78.1 in baseline vs. 29.8 in DFM). This heterogeneity indicates that the economic costs of model misspecification may not be evenly distributed across sectors but concentrated among systemically important sectors.

Overall, Section 3 establishes that cross-sectoral spillovers account for approximately 40% of total price variation, substantially exceeding the contribution of aggregate factors. The baseline model provides reliable estimates by avoiding the systematic biases of restricted specifications: pure VAR models overestimate spillovers by conflating aggregate comovements with direct transmission, while DFM specifications underestimate spillovers by assuming independent idiosyncratic dynamics. Having established the magnitude of spillovers, the analysis now turns to examining which specific sectors drive these transmission patterns.

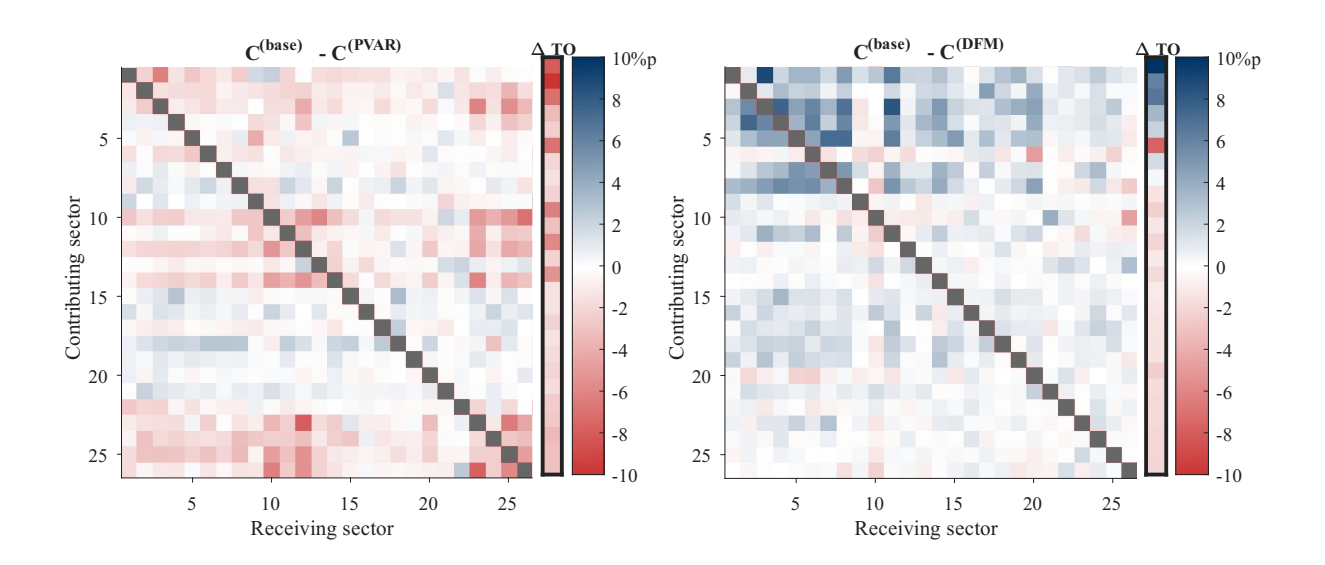


Figure 5: Model Differences in Sectoral Spillover Estimates

Notes: (a) This figure shows difference matrices between the baseline model and benchmark specifications. Left panel: Baseline minus PVAR differences. Right panel: Baseline minus DFM (B=0) differences. (b) Color scale ranges from -10 percentage points (dark red, baseline estimates lower) to +10 percentage points (dark blue, baseline estimates higher). Sectors are reordered so the highest spillover transmitters based on the weighted TO index appear first (top rows/left columns). (c) The ΔTO bars show differences in weighted TO indices between models for each sector. Positive values indicate the baseline model estimates higher transmission than the comparison model.

4 Granularity in Sectoral Spillover Patterns

Building on the evidence that spillovers are quantitatively substantial, this section identifies which sectors act as key transmission hubs and examines how alternative model specifications affect sectoral rankings. The granular structure of spillovers has important implications for policy monitoring and macroeconomic modeling.

4.1 Identifying Key Transmission Hubs

This subsection identifies which sectors act as central nodes in driving cross-sectoral spillovers under the baseline model. Figure 6 illustrates the spillover structure over a 16-quarter horizon using spring-embedded network graphs, highlighting the sectors that occupy key positions within the transmission network.

The NET network (left panel) identifies dominant transmission hubs using the NET index, which classifies sectors as net transmitters or net absorbers in balanced quintiles. The top quintile, shown in dark blue with the largest node sizes, includes the strongest net transmitters: food (51.1), furnishings (36.5), food services (30.9), personal care (22.2), and other services (20.2). Gasoline falls into the second category (medium blue) as a moderate net transmitter, consistent with its relative insulation from spillovers originating in other sectors. These leading sectors exhibit the highest net directional connectedness: shocks originating in them propagate strongly to the rest of the system while remaining comparatively insulated

¹⁵All reported net spillover indices correspond to the variance decomposition results presented in Table C5.

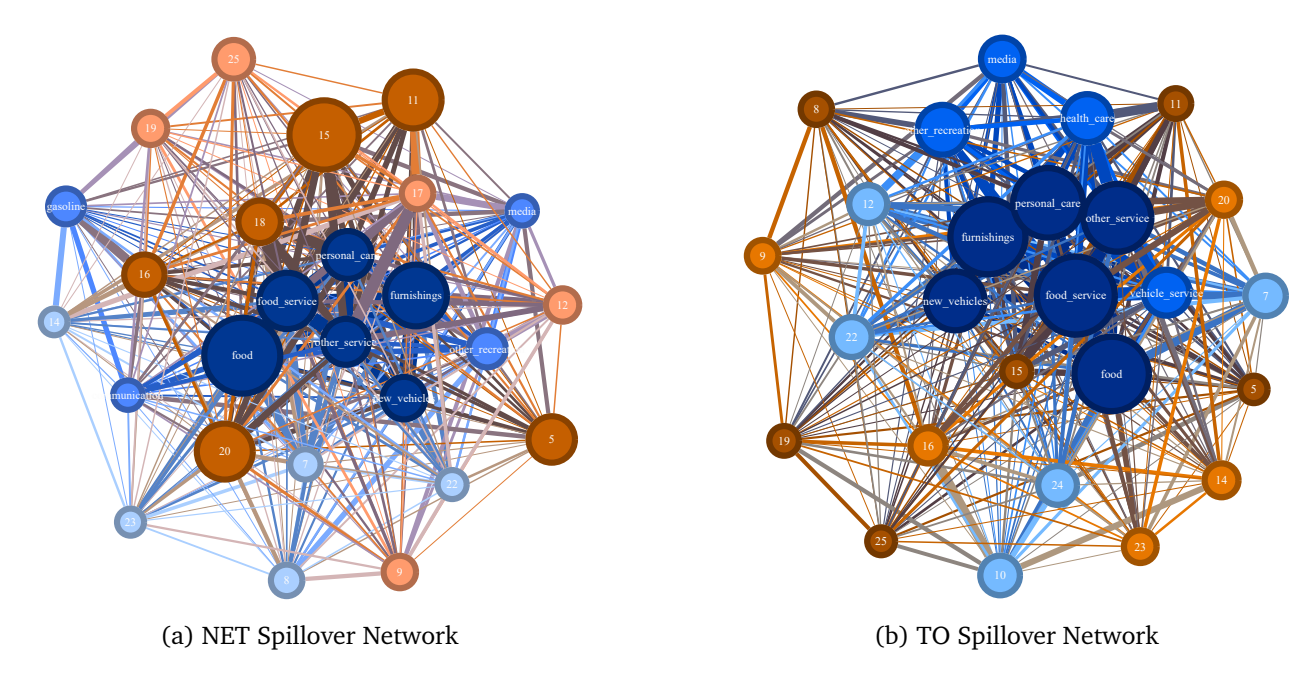


Figure 6: Network Visualization of Sectoral Spillover Structure

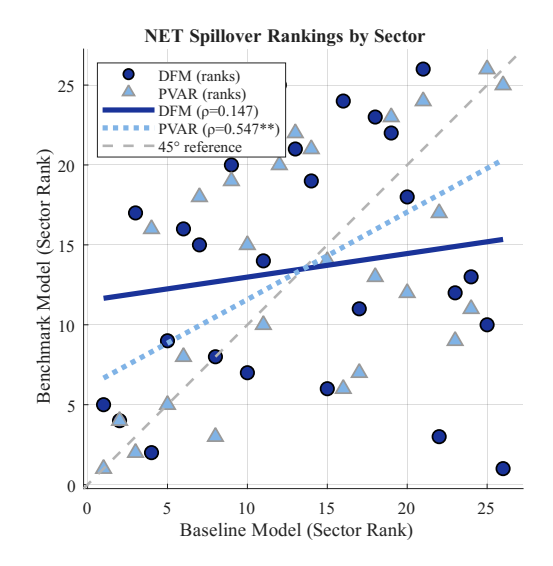
Notes: (a) This figure presents network spring graphs visualizing the baseline model's spillover structure. Left panel: NET spillover network based on net directional connectedness, Right panel: TO spillover network based on size-weighted total directional connectedness. (b) Larger size and darker color of nodes reflect higher intensity of spillovers. Nodes are colored dark blue for top 20% net transmitters, transitioning to the bottom 20% net absorbers in dark orange. (c) Edge thickness represents pairwise connectedness strength. (d) The spring layout positions strongly connected sectors closer together using FortAtlas2 algorithm.

from external influences.

The TO network (right panel) highlights size-weighted transmission capacity. Core transmitters from the NET network remain dominant, while gasoline (node 10) drops to the middle quintile due to moderate transmission intensity and a smaller consumption share. Service-sector clustering reflects underlying labor and business linkages, and food-related categories remain central across both networks. When weighted by sector size, health care moves up the ranking. Although the health care sector is a net absorber—receiving more shocks than it transmits—it still generates notable outward spillovers. Its higher prominence in the size-weighted TO network stems from the interaction of these spillovers with its large sectoral share and strong idiosyncratic dynamics. In contrast, food and food services combine both substantial net transmission capacity and significant size. Overall, the TO network demonstrates how sectoral scale and network linkages jointly determine aggregate spillovers.

Gasoline exhibits a distinctive spillover profile that highlights the asymmetry of sectoral interconnections. Although its total transmission is only moderate compared with leading categories such as food, it nonetheless registers as a net contributor even over a 16-quarter horizon. This persistence is noteworthy since gasoline is typically regarded as a transitory component of inflation. Gasoline's persistent net transmission may reflect its role as both an intermediate input and final consumption good, with shocks potentially propagating downstream through transportation costs and production chains while remaining relatively insulated from domestic demand spillovers. At the same time, these shocks propagate strongly

¹⁶Numerical values in Table C5 report unweighted connectedness; the TO indices shown here are additionally weighted by sectoral consumption shares.



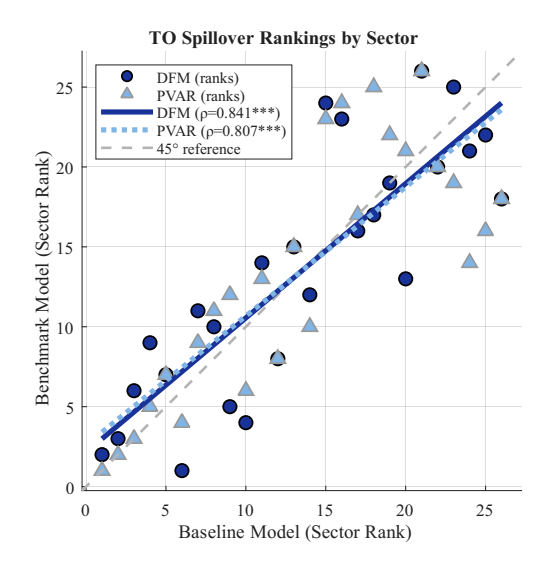


Figure 7: Cross-Model Consistency in Sectoral Spillover Rankings

Notes: (a) This figure compares sectoral rankings between the baseline model and benchmark specifications. Left panel: NET spillover rankings comparing sectors' net transmission roles. Right panel: TO spillover rankings based on total contributions weighted by consumption shares. (b) Each point represents one sector's ranking across models. The 45-degree reference line indicates perfect rank agreement. DFM comparisons use circles with solid trend lines; PVAR comparisons use triangles with dotted trend lines. (c) Spearman rank correlation coefficients (ρ) and significance levels are shown in legends. (d) Deviations from the line indicate that modeling choices affect the identification of key sectors in the network.

downstream through transportation costs and production chains, producing a positive net index despite moderate overall transmission.

By contrast, the dominant net transmitters—food, food services, furnishings, and personal care—are primarily shaped by strong upstream exposure to final demand, while also transmitting shocks downstream into related sectors. For example, food acts both as a staple consumption category with relatively inelastic demand and, through its use in food services and other production activities, as an intermediate input, allowing shocks to spill over through consumption as well as production linkages. Food services, while reliant on food inputs, function chiefly as a final consumption sector, with potential transmission channels that warrant further investigation. Furnishings and personal care, meanwhile, can be viewed as more discretionary categories, where demand-driven shocks spread through substitution effects and household budget reallocations, while their downstream spillovers into production chains remain comparatively limited.

4.2 Model Consistency in Sectoral Rankings

A natural question is whether the two benchmark models identify the same central sectors as the baseline. If they did, the choice of modeling framework would matter less for sectoral analysis. In practice, however, the differences are substantial. This subsection examines the sources of these discrepancies by analyzing both the propagation mechanics of the transition matrix and the heterogeneity in factor sensitivity across sectors.

Figure 7 compares sectoral rankings across models for both net and total spillover contributions. First, for NET spillover rankings (left panel), the Spearman correlations with the baseline are moderate: $\rho=0.55$ for the PVAR and only $\rho=0.15$ for the DFM. These results show that conventional models frequently misclassify which sectors act as net transmitters versus net absorbers, reflecting fundamental differences in how sectoral comovement is attributed across frameworks. Models that do not disentangle aggregate factors from direct cross-sectoral dynamics systematically distort the roles that sectors play in the transmission network.

For TO spillover rankings (right panel), correlations are somewhat higher ($\rho = 0.81$ for PVAR, $\rho = 0.84$ for DFM), but the scatter around the 45-degree line shows persistent disagreement about which sectors are the strongest transmitters. This suggests that model choice matters not only for aggregate measures but also for sectoral targeting, with potential implications for policy monitoring and intervention.

These discrepancies in sectoral rankings arise from two sources: (i) differences in how models capture cross-sectoral transmission dynamics through the transition matrix *B*, and (ii) differences in how variance is attributed between aggregate factors and idiosyncratic sectoral shocks. The following sub-sections examine each channel in turn.

4.2.1 Propagation Dynamics of the Transition Matrix

First, Figure 8 illustrates the transition matrices underlying the spillover estimates, highlighting fundamental differences in how alternative model specifications capture cross-sectoral transmission channels.¹⁷ The discussion proceeds along four complementary dimensions: (i) sparsity and selection patterns, (ii) magnitude of spillover coefficients, (iii) persistence, and (iv) concentration across sectors.

Sparsity and Selection Patterns. – The baseline model retains 29 of 52 diagonal elements (55.8%)—reflecting within-sector persistence—and 165 of 1,300 off-diagonal elements (12.7%)—reflecting cross-sector spillovers. By contrast, the PVAR is the densest, with 34 diagonals (65.4%) and 225 off-diagonals (17.3%), while the DFM is the sparsest, with only 23 diagonals (44.2%) and 78 off-diagonals (6.0%). The baseline's pattern reflects the model's ability to preserve strong own-sector dynamics while isolating a plausible set of spillover channels, avoiding over-parameterization. The PVAR overstates linkages because its *B* estimates has to absorb both persistence and common comovements, forcing LASSO to select spurious links. The DFM, in turn, compresses residual dynamics into a sparse structure, since much of the comovement is absorbed by factors in the first step, leaving few spillover channels in the second step.

Link Strength and Conditional Magnitudes. – The baseline model exhibits diagonal link strengths of 0.263 and off-diagonal strengths of 0.119. The PVAR shows slightly lower diagonals (0.227) and the weakest off-diagonals (0.111), while the DFM yields the strongest diagonals (0.273) and the strongest off-diagonals (0.146). This confirms that own-sector effects dominate cross-sector propagation in all models, but with different emphases: the PVAR spreads propagation thinly across many links, the DFM concentrates weight on a small set of residual spillovers, and the baseline avoids both extremes, preserving moderate link strengths in a plausibly diffuse structure.

 $^{^{17}}$ In the baseline and PVAR models, the transition matrix for sectoral propagation is taken directly from the estimated coefficients in the first step. In the DFM model, where the B=0 restriction rules out direct propagation by construction, the transition matrix is instead inferred from the dynamics of the residuals in the second step of the two-step procedure. In all cases, the resulting object captures the mechanics of sectoral shock transmission, though obtained under different model restrictions.

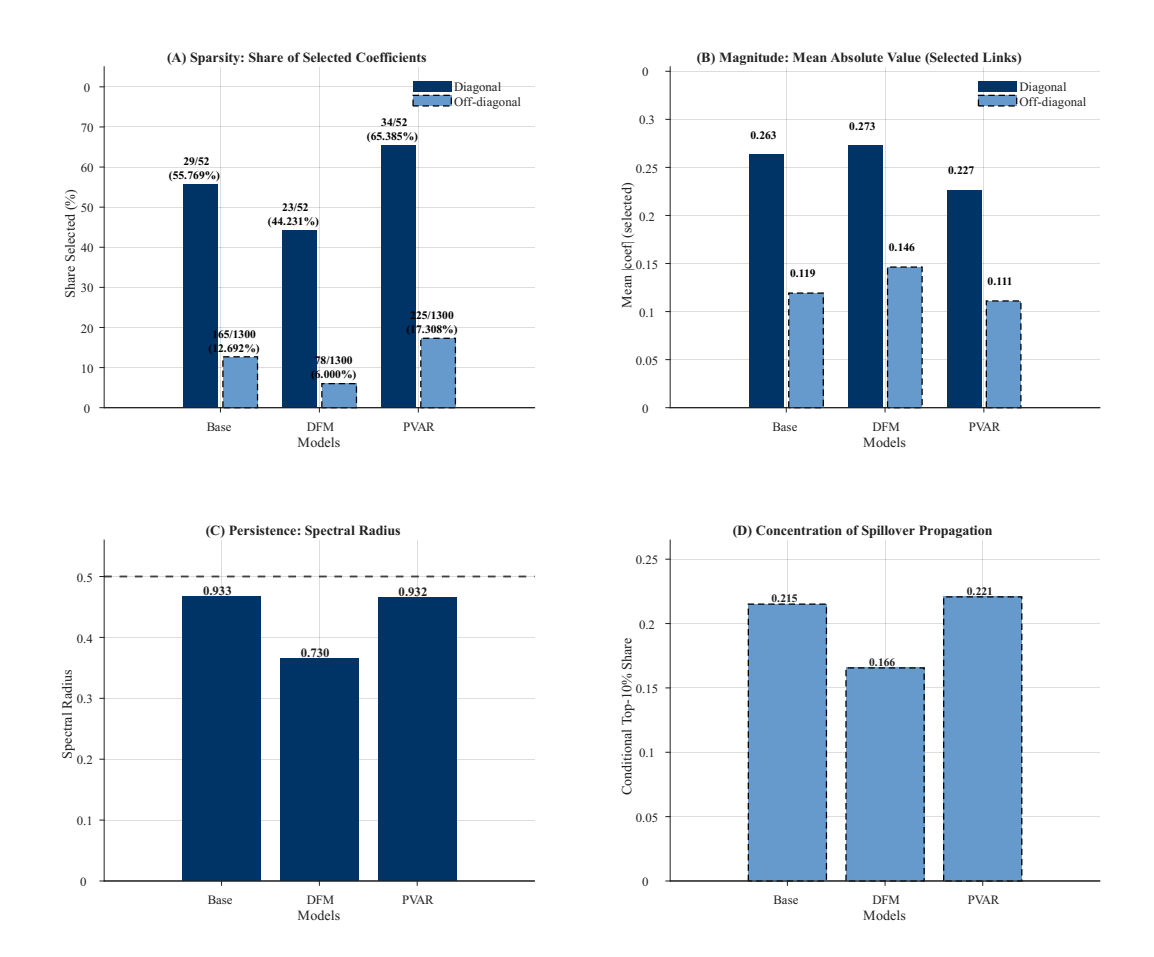


Figure 8: Propagation Mechanics Across Model Specifications

Notes: This figure analyzes the propagation mechanisms captured by the estimated transition matrices across three model specifications, focusing on the top half of the B matrix for prices. (a) Panel A shows sparsity patterns: diagonal bars (dark blue) represent the share of own-sector effects selected by LASSO, while off-diagonal bars (medium blue with dashed borders) show cross-sectoral linkage selection rates. Numbers indicate counts and percentages of selected coefficients. (b) Panel B displays link strength: mean absolute values of selected diagonal and off-diagonal coefficients, with values shown to three decimal places. (c) Panel C presents spectral radius measures indicating persistence potential, with the dashed line at 1.0 marking the stability threshold. (d) Panel D shows concentration measures: the conditional top-10% share of total spillover strength among selected off-diagonal links, measuring whether propagation is hub-dominated or diffuse.

Persistence. – The baseline and PVAR models both show high persistence, with spectral radii of 0.933 and 0.932 respectively, while the DFM model is lower at 0.730. The baseline model's persistence reflects the combined influence of factor-driven and idiosyncratic propagation channels. The PVAR model exhibits similarly high persistence, though this partly reflects common comovements being absorbed into the *B* matrix. By contrast, the DFM model records lower persistence, since the restriction shifts dynamics into the factor component, leaving the residual dynamics comparatively weak.

Concentration and Hub Structure. – The baseline model records moderate concentration (0.215), the PVAR slightly higher (0.221), and the DFM considerably lower (0.166). These differences imply distinct network architectures: the baseline highlights systematically important hubs with balanced concentration; the PVAR model produces a marginally more hub-dominated structure; and the DFM model yields a more diffuse network, with spillovers spread more evenly across sectors. Such contrasts show that model choice affects not only overall spillover intensity but also the identification of systemic hubs.

Synthesis. – Across all four dimensions, the baseline provides a balanced characterization of cross-sectoral propagation—sparser and more selective than the PVAR, yet richer and more persistent than the DFM. These system-wide properties set the stage for the analysis of sectoral granularity, where differences in propagation mechanics translate into heterogeneous sectoral rankings.

4.2.2 Heterogeneity in Factor Sensitivity

Second, Figure D2 extends the variance decomposition analysis to the individual sector level, revealing substantial heterogeneity in factor sensitivity that varies systematically across model specifications. The baseline model (center panel) shows that aggregate factor sensitivity ranges from approximately 6.5% for highly idiosyncratic sectors like alcohol to 31.4% for sectors most exposed to economy-wide conditions like accommodations. Other sectors with high aggregate sensitivity include garments (30.5%), finance (27.5%), and gasoline (27.9%), while sectors like personal care (19.4%), other services (10.6%), and medical (9.4%) show lower sensitivity.

The PVAR model, by construction, assigns zero variance to aggregate factors, attributing all comovement to direct propagation. This uniform treatment eliminates sectoral heterogeneity in factor sensitivity, flattening differences across categories and obscuring which sectors are genuinely more or less exposed to aggregate shocks. The absence of this heterogeneity also contributes to distortions in sectoral rankings within the network.

By contrast, the DFM model systematically inflates aggregate shares in many sectors. This effect is particularly pronounced for those that serve as important transmission hubs in the baseline model—precisely where cross-sectoral spillovers are strongest. For example, vehicle services shows aggregate shares of 67.5% in DFM versus 14.9% in baseline, while food services exhibits 67.2% versus 13.9%, and other services 60.7% versus 10.6%. In such cases, the DFM absorbs spillover-driven dynamics into its factor estimates, creating the impression that these sectors are primarily driven by aggregate forces when in fact they act as conduits for cross-sectoral transmission. ¹⁸

¹⁸Although inflation of factor shares is the dominant pattern, a few sectors (e.g., gasoline, finance, education, communication, tobacco) instead show lower aggregate shares in DFM relative to the baseline. This reflects how the DFM restriction eliminates spillover propagation and reallocates comovement into the factor structure: spillover-driven sectors become more closely aligned with the factors, while others lose alignment and thus record lower factor shares.

Overall, the sectoral-level comparison reinforces the earlier finding that joint modeling is essential: conventional approaches not only bias aggregate spillover measures but also systematically mischaracterize which sectors are most important for propagating shocks.

The empirical patterns in Sections 3 and 4 establish the magnitude and distribution of spillovers but leave open the mechanisms through which they arise. While the baseline model provides more reliable estimates of magnitudes and sectoral rankings—an assessment reinforced by the robustness checks and extensions in Section 6—it does not identify whether the observed propagation reflects production linkages, sectoral heterogeneity, or other channels. To shed light on these mechanisms, the next section interprets the baseline findings through the lens of a multisector model.

5 Theoretical Mechanisms and Empirical Tests

This section complements the empirical results by using the multisector model of Pasten et al. (2024) as a conceptual lens. Rather than a structural estimation, the aim is to interpret the documented spillovers through the mechanisms highlighted by the model: sectoral shocks propagate via production linkages and are shaped by various frictions and sectoral heterogeneities. I present the key analytical result as a benchmark and evaluate its predictions using dyadic regressions of pairwise connectedness on network linkages, sector size, and nominal rigidity.

5.1 Theoretical Foundations and Bridge to Empirics

The model features K monopolistically competitive sectors. Households aggregate sectoral goods into final consumption with weights $\Omega_c = (\omega_{c1}, \ldots, \omega_{cK})$. Firms combine labor and intermediate inputs using Cobb–Douglas technology, where the input–output (IO) weights are $\Omega = \omega_{kk'k,k'}$ and δ is the intermediate-input share. Prices adjust according to sector-specific Calvo frictions, summarized by Λ .

Simplifying assumptions leading to the baseline multiplier. – The simplest form of the sectoral multipliers is derived under four assumptions: (i) log utility and linear disutility of labor ($\phi = 0$), implying an integrated labor market with infinitely elastic supply and nominal wages proportional to nominal GDP; (ii) nominal GDP targeting ($p_t^c + c_t = 0$), which fixes wages in steady state; (iii) information-based price rigidity, whereby sector k sets its price with probability λ_k before observing shocks; and (iv) i.i.d. sectoral productivity shocks a_{kt} with identical variance, which make the pricing problem static. Under these assumptions, the sectoral multiplier takes the form:

$$p_t^c = -\chi' a_t, \qquad \chi \equiv (\mathbf{I} - \Lambda) (\mathbf{I} - \delta \Omega' (\mathbf{I} - \Lambda))^{-1} \Omega_c,$$
 (13)

Equation (13) makes transparent that sectoral multipliers depend on three elements: (i) the *production* network structure (Ω) and the intermediate-input share (δ) (ii) sector size in final demand (Ω_c); and (iii) nominal rigidity (Λ).¹⁹

Persistence adjustment. - Replacing information-based price rigidity with Calvo pricing frictions and

¹⁹Here, p_{kt} are log-linear deviations of prices from steady state, and inflation is defined as $\pi_{kt} = p_{kt} - p_{k,t-1}$. The static relationships, as summarized from from Pasten et al. (2024), illustrate the link between sectoral multipliers, production-network parameters, sectoral size, and nominal rigidities. The formally derived dynamics with Phillips curves are provided in Rubbo (2023).

allowing for autoregressive persistence $\rho_k > 0$ in sectoral shocks yields a persistence-adjusted multiplier:

$$\chi_k^{(\rho)} = \sqrt{\sum_{\tau=0}^{\infty} \rho_k^{2\tau}} \, \chi_k,\tag{14}$$

which parallels the multi-horizon dynamic sectoral spillover measure in the empirics.

Labor-market segmentation ($\phi > 0$). – Relaxing the simplifying assumption of linear disutility of labor ($\phi = 0$) to allow a positive inverse Frisch elasticity $\phi > 0$ makes wages partly demand-determined:

$$w_{kt} = c_t + p_t^c + \phi \, \ell_{kt}^d. \tag{15}$$

Labor markets then become segmented, and sectoral productivity shocks affect wages via sector-specific labor demand, opening an additional propagation channel. In particular, shocks can propagate *upstream* because labor demand depends on demand for inputs from downstream sectors. The $K \times 1$ vector of multipliers χ solves

$$\chi = \left[\mathbf{I} + (1 - \delta) \phi \Theta^{-1}\right] (\mathbf{I} - \Lambda) \left\{\mathbf{I} - \delta \Omega' (\mathbf{I} - \Lambda) - (1 - \delta) \left(\theta_p' - \Omega_c \theta_c'\right) (\mathbf{I} - \Lambda) \Theta^{-1}\right\}^{-1} \Omega_c, \tag{16}$$

where

$$\Theta \equiv (1 + \delta \phi)\mathbf{I} - (1 + \phi)\psi D\Omega D^{-1}, \tag{17}$$

$$\theta_c \equiv \left(\mathbf{I} - \psi D^{-1} \Omega' D\right) \iota + \phi (1 - \psi) D^{-1} \Omega_c, \tag{18}$$

$$\theta_{p} \equiv \left(\mathbf{I} - \psi D^{-1} \Omega' D\right) \iota \Omega'_{c} - \phi \, \eta \left[\mathbf{I} - (1 - \psi) D^{-1} \Omega_{c} \Omega'_{c}\right] + \phi \left[(\eta - 1) \psi D^{-1} \Omega' D \Omega - \delta \Omega \right].$$
(19)

Here, $D = \operatorname{diag}(n_k)$ contains sector sizes, ψ is the steady-state intermediate-input share, and ι is a vector of ones. The upstream supplier is indexed k and the downstream buyer k'. With $\phi > 0$ —capturing segmented labor markets—sectoral size enters *inside* the propagation operator via D and D^{-1} , which induces directional size tilts in both forward and backward transmission. In particular,

$$(D\Omega D^{-1})_{k,k'} = \frac{n_k}{n_{k'}} \Omega_{k,k'}$$
 and $(D^{-1}\Omega' D)_{k,k'} = \frac{n_{k'}}{n_k} \Omega_{k',k}$.

Relative size tilts transmission in opposite directions: forward links scale with $(D\Omega D^{-1})_{k,k'} = (n_k/n_{k'})\Omega_{k,k'}$, while backward links scale with $(D^{-1}\Omega'D)_{k,k'} = (n_{k'}/n_k)\Omega_{k',k}$. With $\phi > 0$, sector size thus loads directly into the propagation operator, reweighting link strengths before aggregation: large suppliers amplify forward transmission toward smaller buyers, and large demanders amplify backward transmission toward upstream suppliers. Equivalently, the same ratios imply attenuation in the opposite direction: when the buyer is large relative to the supplier $(n_{k'}\gg n_k)$, forward transmission from the small supplier is dampened; when the supplier is large relative to the demander $(n_k\gg n_{k'})$, backward transmission from the small demander is dampened.

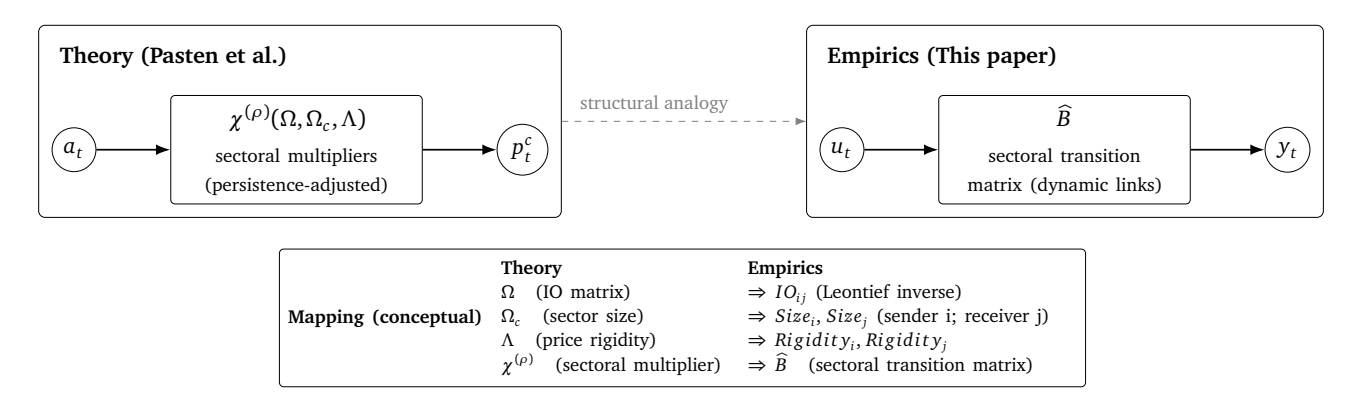


Figure 9: THEORY-EMPIRICS BRIDGE

Note: Theoretical flow $a_t \to \chi^{(\rho)}(\Omega, \Omega_c, \Lambda) \to p_t^c$ corresponds conceptually to the empirical flow $u_t \to \widehat{B} \to y_t$. While the theoretical multiplier $\chi^{(\rho)}$ is derived from a fully specified structural model with aggregates and multiple sectoral variables, the empirical VAR is parsimonious—estimated directly from sectoral prices and consumption without aggregates or a priori structural restrictions. This difference in scope means the mapping is not one-to-one, but \widehat{B} still provides a reduced-form measure of dynamic network propagation that can be compared with theoretical predictions.

Bridge to empirics. – Having established the model's structure and the role of persistence-adjusted multipliers $\chi^{(\rho)}$, I now connect these theoretical objects to the empirical framework. the baseline empirical specification is a high-dimensional VAR with common factors, which I have used throughout the paper to measure sectoral interdependencies directly from the data. The VAR includes only sectoral prices and consumption, excluding aggregates to mitigate multicollinearity concerns, and is therefore far more parsimonious than the theoretical model—which incorporates aggregate variables and a wider set of sectoral variables such as productivity and wages. Nonetheless, it offers a flexible, data-driven benchmark against which I can assess how closely the empirical propagation patterns align with the model's predictions.

Figure 9 illustrates the conceptual mapping between the theoretical framework and its empirical implementation. In theory, the input–output production linkages Ω , sector sizes Ω_c , and nominal rigidities Λ jointly determine the persistence-adjusted multiplier $\chi^{(\rho)}$, which maps sectoral productivity shocks a_t into aggregate prices p_t^c . In the empirical VAR, the estimated sectoral transition matrix \widehat{B} plays an analogous role, mapping sectoral shocks u_t^{20} to sectoral outcomes y_t . Although the mapping is not one-to-one, the empirical analysis employs observed counterparts to the theoretical parameters: measures of input–output linkages, sectoral size, and price rigidity serve as proxies for Ω , Ω_c , and Λ , respectively. Comparing $\chi^{(\rho)}$ with the \widehat{B} -implied network effects in the connectedness matrix DY_p then provides a way to assess the degree of empirical alignment with the theoretical transmission structure.

5.2 Testing Theoretical Predictions: Dyadic Regression Analysis

A natural benchmark is to assume that the connectedness matrix mirrors the input–output (IO) matrix without frictions. In contrast, the approach does not impose this assumption. Instead, I estimate spillover networks directly from the data and then test whether the resulting patterns align with theoretical mechanisms that incorporate not only production linkages but also pricing frictions and sectoral heterogeneities. This methodology allows us to assess what the data reveal about sectoral interconnectedness beyond mechanical IO propagation, while also testing the richer framework of Pasten et al. (2024), which emphasizes the role

²⁰Sectoral shocks are identified using generalized impulse responses from sectoral prices and consumption. These shocks are not structural supply or demand disturbances, but composite innovations capturing correlated movements in prices and consumption.

of nominal rigidities, sector size, and other frictions alongside production networks.

The analysis tests six specific hypotheses about the determinants of spillover magnitude from sector i to sector j:

H1 (Forward links): Spillover increases with downstream input-output requirement from sector i to sector j.

H2 (Backward links): Spillover increases with the share of sector *i*'s output sold to downstream sector *j*.

H3 (Sender size): Spillover effects vary with the economic size of the sending sector i.

H4 (Receiver size): Spillover effects vary with the economic size of the receiving sector j.

H5 (Sender rigidity): Spillover effects vary with the degree of price rigidity in the sending sector i.

H6 (Receiver rigidity): Spillover effects vary with the degree of price rigidity in the receiving sector j.

Empirical Specification. - The dyadic regression framework models pairwise connectedness as:

$$DYp_{ij} = \alpha + \beta_1 IO_{ij} + \beta_2 ShareOut_{ij} + \gamma'(IO_{ij} \times X_{ij}) + \delta'(ShareOut_{ij} \times X_{ij}) + \mu_i + \nu_j + \varepsilon_{ij}$$

where DYp_{ij} is the Diebold–Yilmaz pairwise connectedness—the share of forecast-error variance in sector j explained by shocks from sector i over a 16-quarter horizon. Direction is defined at the dyad level: IO_{ij} traces forward (downstream) production links with i as supplier and j as buyer, while $ShareOut_{ij}$ traces backward (upstream) demand links with i as seller and j as supplier. Coefficients therefore quantify how cross-sectional differences in relative dyadic spillover intensity align with these forward/backward linkages, and how that alignment varies with sectoral traits X_{ij} . Sender (μ_i) and receiver (ν_j) fixed effects absorb level differences in sectors' propensities to transmit or receive shocks; identification comes from within-sender and within-receiver variation across dyadic partners.

I construct IO_{ij} as the column-normalized technical coefficient from the bridge-matrix–transformed BEA input–output tables, and $ShareOut_{ij}$ as the row-normalized share of sector i's total sales to sector j, based on the same transformed flows. These variables capture the forward and backward linkage channels. The sector-level covariates X_{ij} include expenditure shares in total PCE ($Size_i$ and $Size_j$) and price-change–frequency–based measures of nominal rigidity derived from microdata ($Rigidity_i$ and $Rigidity_j$). All regressors are standardized to have zero mean and unit variance, allowing coefficients to be interpreted as the effect of a one–standard–deviation change. The interaction terms then capture how the effects of IO_{ij} and $ShareOut_{ij}$ vary systematically with sectoral heterogeneity (H3–H6).

Results. – Table C6 reports estimates that reveal both alignment with and departures from simple input–output predictions. Column (1) provides a baseline test of whether cross-sectional variation in dyadic connectedness corresponds solely to production-network linkages. The coefficient on IO_{ij} —measuring forward or downstream technical requirements—is 2.027 (s.e. 0.880), indicating that a one–standard–deviation increase in IO_{ij} is associated with a statistically significant 2.0 percentage point rise in DYp_{ij} , consistent with H1.

Importantly, the coefficient on $ShareOut_{ij}$ —which captures backward or upstream sales-share linkages—is 3.654 (s.e. 0.790) and highly significant, providing strong support for the second hypothesis (H2). This result indicates that empirical spillovers reflect upstream market concentration effects. The positive coefficient implies that sectors selling a larger share of their output to specific buyers are more exposed to those buyers' shocks, generating stronger upstream spillovers through demand-driven transmission channels that complement the downstream effects observed in production networks.

These empirical patterns are consistent with broader evidence on demand-driven propagation. Das et al. (2022) show that demand shocks generate larger spillovers than supply shocks in output-based analyses, primarily through upstream linkages from customer to supplier sectors. Similarly, Luo and Villar (2023) find that while supply-side TFP shocks propagate strongly downstream, demand-side trade shocks propagate in both directions—upstream and downstream—consistent with the mechanisms identified here. Columns (2)–(7) reveal additional complexities that distinguish empirical spillovers from mechanical IO propagation. For sender size effects (H3), the downstream linkage interactions ($IO_{ij} \times Size_i$) are consistently negative and highly significant across specifications, with coefficients ranging from -1.676 to -1.221. This pattern indicates that, when sector i acts as the upstream supplier in a dyad, the alignment between technical input requirements and observed downstream spillover intensity tends to weaken as the sender becomes larger. For receiver size effects (H4), the downstream-linkage interactions ($IO_{ij} \times Size_j$) are positive (0.560 to 1.409) but significant only in specifications (3) and (7). Together, these results indicate asymmetric size effects in downstream propagation between senders and receivers.

For backward (upstream) links, similar asymmetries appear. The $ShareOut_{ij} \times Size_i$ coefficient is positive (1.274 in column 3, 0.520 in column 7) in two specifications, suggesting that the association between relative spillover intensity DYp_{ij} and buyer concentration ($ShareOut_{ij}$) tends to be stronger when the sending sector i is larger. In contrast, the $ShareOut_{ij} \times Size_j$ coefficient is consistently negative and highly significant (-2.180 in column 3, -2.423 in column 7), indicating that this association diminishes as the receiving sector j becomes larger. These asymmetries imply that spillover intensity varies systematically with sector size on both sides of the linkage, though the underlying mechanisms cannot be directly inferred from these estimates.

For pricing rigidity effects (H5–H6), the results show limited and statistically weak evidence. The downstream rigidity interactions ($IO \times Rigidit y_i$ and $IO \times Rigidit y_j$) display mixed signs and lack statistical significance, with coefficients ranging from -1.268 to 1.101 across specifications. Similarly, the upstream rigidity interactions ($ShareOut \times Rigidit y_i$ and $ShareOut \times Rigidit y_j$) vary in sign and magnitude—from -0.002 to 0.942—but remain insignificant throughout. This specification sensitivity indicates that pricing-rigidity effects, for both downstream and upstream linkages, are weak over the horizons considered and contribute little to explaining persistent spillovers.

Model Selection and Specification Sensitivity. – The progression across specifications provides useful insights into robustness. While the core network effects and size interactions remain stable, the price-rigidity effects and certain size interactions vary across models. To identify the preferred specification, I conduct nested F-tests and evaluate the Bayesian Information Criterion (BIC). Both criteria support retaining only the size-interaction terms, with specification (3) offering the best overall fit among the nested alternatives.

Figure 10 presents the coefficient estimates and confidence intervals for the preferred specification (3). The results confirm positive main effects of both forward and backward linkages, along with significant negative forward sender–size interactions ($IO_{ij} \times Size_i$) and backward receiver–size interactions ($ShareOut_{ij} \times Size_j$). In contrast, the forward receiver–size ($IO_{ij} \times Size_j$) and backward sender–size ($ShareOut_{ij} \times Size_i$) interactions are positive but only marginally significant.

Assessment: Evidence for Departures from Frictionless IO Models. – The results provide evidence that empirical spillover patterns extend beyond what would be predicted by frictionless input–output models,

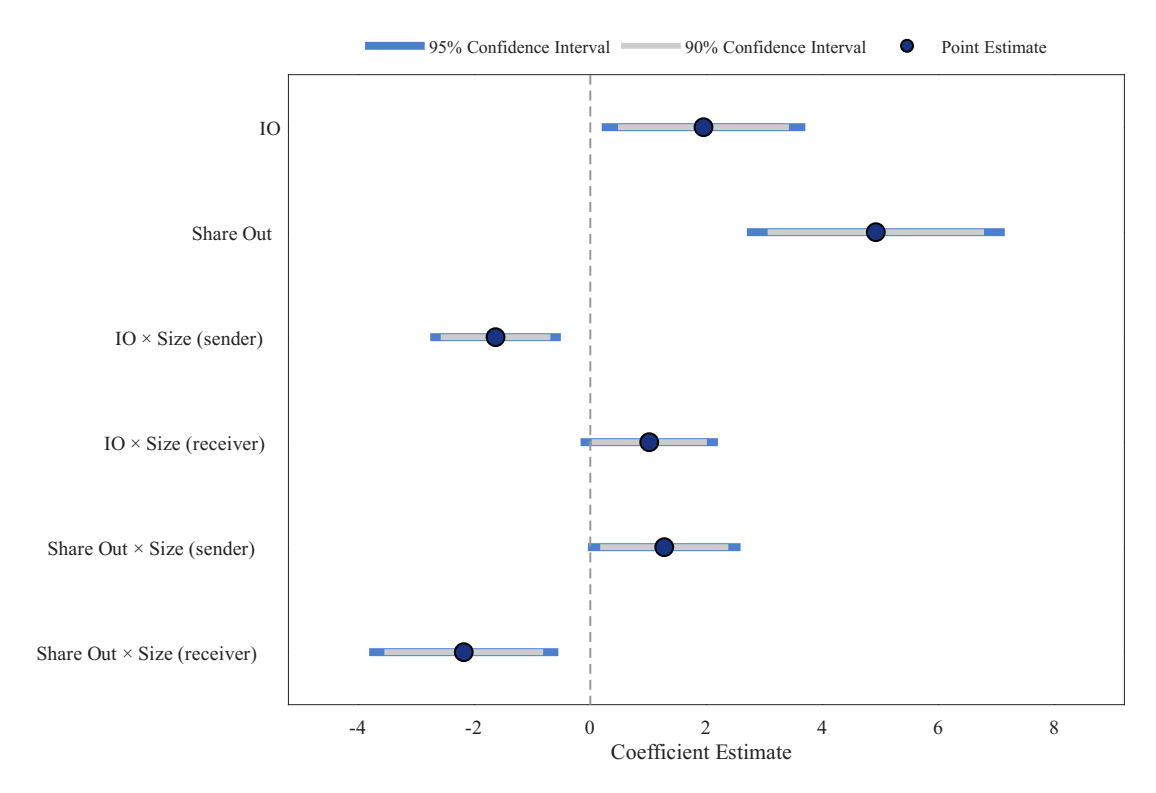


Figure 10: DYADIC REGRESSION COEFFICIENT ESTIMATES

Notes: This figure visualizes the dyadic fixed effects regression results: (a) The dependent variable is the Diebold–Yilmaz pairwise connectedness for sectoral prices, DY_{ij}^P , defined as the share of forecast-error variance of sector j's inflation explained by shocks from sector i (ordered dyads). (b) The model includes two-way fixed effects for sender (i) and receiver (j). (c) Coefficient estimates are plotted with 90% (gray) and 95% (blue) confidence intervals, based on heteroskedasticity-robust standard errors clustered by sender, for specification (3) in Table C6. (d) All regressors are standardized, so coefficients represent the effect of a one–standard-deviation change. (e) Dyadic regressors: IO_{ij} (input requirement from i to j) and $ShareOut_{ij}$ (fraction of i's output sold to j). Sector characteristics: $Size_i$, $Size_j$ (sectoral sizes). Price rigidity terms ($Rigidity_i$, $Rigidity_j$) are omitted as statistically insignificant. Interaction terms allow IO and ShareOut effects to vary with sector size.

while showing selective alignment with mechanisms featuring sectoral heterogeneity. Robust support emerges for both H1 (downstream linkages) and H2 (upstream market shares), with these relationships stable across specifications: the 2.0 percentage point IO_{ij} effect and the 3.7 percentage point $ShareOut_{ij}$ effect indicate economically meaningful propagation through both downstream and upstream channels.

Beyond the main effects, the size interaction terms related to H3 and H4 also reveal departures from a mechanical IO mapping. In the *forward* block, a pure forward size–tilt would predict amplification for large suppliers and attenuation for large buyers. the estimates instead show $IO_{ij} \times Size_i < 0$ and $IO_{ij} \times Size_j > 0$, indicating a departure from a purely forward size–tilt. By contrast, the backward block aligns with the size–tilt prediction: $ShareOut_{ij} \times Size_i$ is positive in restricted specifications, and $ShareOut_{ij} \times Size_j < 0$. This combination is consistent with the segmented-labor operator's size tilts for upstream (demand-driven) propagation. Taken together, the sign reversal in the IO block and the theory-congruent signs in the ShareOut block suggest that size mediates dyadic alignment differently across senders and receivers, with the backward channel appearing more salient in the setting.

There is no evidence supporting H5 or H6 regarding price rigidity interactions. Pricing-rigidity effects remain weak in the chosen specification, suggesting that, over the horizons examined, the size-mediated network structure explains a greater share of the cross-sectional variation in relative dyadic spillovers than nominal stickiness.

Overall, production linkages remain a central organizing framework, but the evidence shows clear departures from a frictionless IO model: Backward channels operate alongside forward ones and their empirical alignment with spillover estimates is mediated by sector size—rather than tracking raw IO coefficients one-for-one.

6 Robustness and Extensions

To ensure that the main findings are not artifacts of model choice, this section presents robustness checks and several extensions. Across specifications, the evidence consistently supports the importance of spillovers and validates the baseline as an economically meaningful middle ground between conventional approaches that either overestimate or underestimate cross-sectoral transmission mechanisms.

6.1 Simulation Evidence

First, to validate the implicit assumption underlying the empirical analysis—namely, that if the true data-generating process involves both common factors and cross-sectoral propagation dynamics, the baseline model can accurately capture these features—this study conducts Monte Carlo simulations across the three model specifications.

The analysis considers a data generating process which includes both common factors and cross-sectoral dynamics. Specifically, it generates a 52-dimensional VAR(1) system with diagonal persistence coefficients of 0.3, sparse off-diagonal spillover coefficients of -0.2 (3 per equation), and factor persistence of 0.6. The performance evaluation considers sample sizes of T = 100, 260, and 2

Figure D3 shows that when both channels are present, the baseline model substantially outperforms the restricted specifications in recovering the true parameters. The DFM produces large, systematic errors in transition matrix recovery, since it imposes a zero matrix and misattributes cross-sectoral effects to factor loadings. By contrast, the PVAR delivers the poorest factor and loading recovery, as it rules out common components and conflates aggregate comovements with direct sectoral linkages. For the baseline, transition matrix errors decline as sample size increases, reflecting consistent recovery of the static parameter. In contrast, errors in the common component time series (Λf_t) naturally grow with sample length, since uncertainty accumulates across more periods.

These results confirm that the baseline provides the most reliable framework when both transmission channels operate, while avoiding the systematic biases that undermine conventional approaches.

6.2 Alternative Specifications

I examine the robustness of main findings to various modeling choices and sample restrictions across five dimensions: factor structure, detrending methods, sample restrictions, outlier treatment, and forecast horizons.

Cross-Specification Stability. – Figure 11 demonstrates consistency across alternative specifications. Results show that the predominance of sectoral dynamics over aggregate factors is robust across specifications, with

²¹This corresponds to the dataset, which spans over 260 quarters, and is representative of typical quarterly macroeconomic samples.

sectoral contributions consistently exceeding 70% of total variance. Moreover, the baseline model maintains intermediate spillover estimates (37%-48%) across all robustness checks, consistently falling between the DFM (B=0) (10%-43%) and higher estimates of the PVAR model (54%-61%). The relative model rankings remain stable across all specifications, confirming that the predominance of sectoral dynamics over aggregate factors is not an artifact of particular modeling choices.

Compared with the baseline spillover estimate of 39.9%, the alternative specifications yield 40% with an additional factor, 48% under global demeaning, 41% in the pre-COVID sample, 43% with outlier adjustment, 37% at an 8-quarter horizon, and 39% at a 12-quarter horizon. These variations reflect economically meaningful differences. The higher estimate under global demeaning (48%) indicates that retaining low-frequency trends amplifies apparent cross-sectoral transmission, as persistent sectoral movements appear more interconnected when trends are preserved. Meanwhile, the pre-COVID restriction (41%) and outlier adjustment (43%) yield results close to the main result, suggesting that pandemic-era volatility was largely captured by the factors in the main model. Finally, spillovers increase from 37% at 8 quarters to 39% at 12 and about 40% at 16, indicating that propagation strengthens with horizon length but stabilizes beyond a three- to four-year window.

Sectoral Robustness and Granularity. – System-wide spillover measures are robust across specifications, but sectoral rankings display greater heterogeneity. In full-sample checks, such as adding factors or adjusting for outliers, the rankings of sectors by TO and NET indices remain highly stable, with Spearman correlations typically above 0.75, confirming that the key transmission hubs are consistently identified. By contrast, the pre-COVID sample, which excludes the volatile 2020–2024 period, produces more reshuffling—particularly among mid-ranked sectors—yielding lower correlations.

At the sectoral level, patterns highlight both consistency and sensitivity in transmission roles. Food and beverages consistently ranks as a strong net transmitter, food services reliably appears among transmitters, and housing emerges as a stable net absorber across specifications. Gasoline, however, is more specification-sensitive: it acts as a stronger transmitter at shorter horizons, as expected, but shifts toward absorption in the pre-COVID sample and under global demeaning. These results align with gasoline's heightened transmission role during the pandemic and the fact that global demeaning retains low-frequency trends—unlike the baseline's local detrending—thereby dampening its estimated net transmission.

6.3 Policy and Broader Implications

The factor-adjusted network approach highlights the importance of jointly modeling aggregate and sectoral dynamics. As demonstrated in the paper's application, conventional frameworks that treat these dimensions separately—such as pure VAR models that tend to overstate spillovers or DFM models that understate them—can distort the relative measured importance of the common factors and the network propagation effects.

A central finding is that, once both influences are accounted for, cross-sectoral spillovers explain roughly two-fifths of total price variation—exceeding the contribution of aggregate factors. This directly addresses the paper's motivating question of whether observed inflation dynamics primarily reflect the diffusion of sector-specific shocks or aggregate disturbances. The evidence indicates that both are important, but that spillovers play a quantitatively larger role, with clear implications for monetary policy design and macroeconomic modeling.

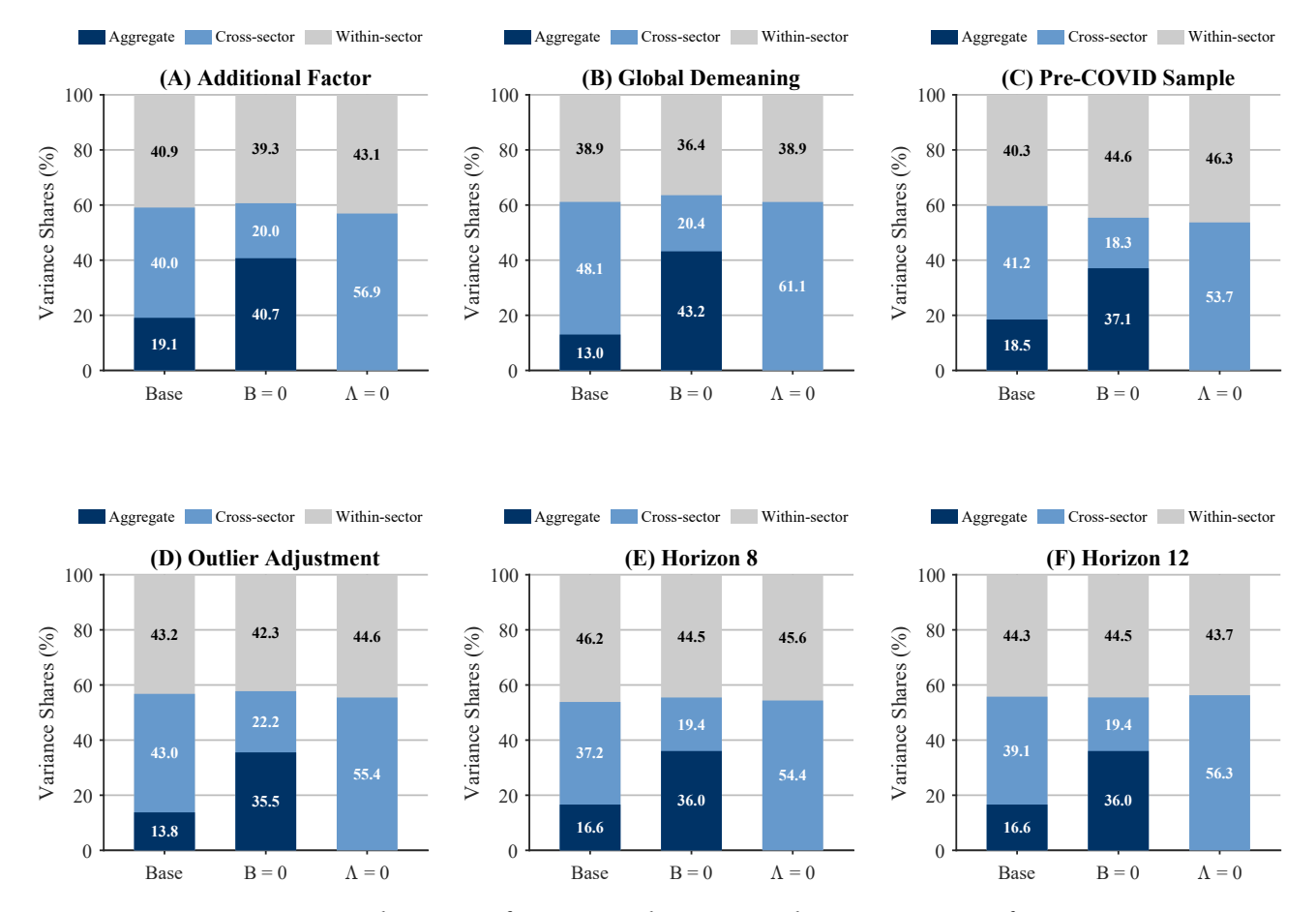


Figure 11: Robustness of System-wide Connectedness Across Specifications

Notes: (a) This figure shows variance decomposition results across alternative specifications for all three model types. Each panel corresponds to different specifications. Panel A: Additional fourth factor specification. Panel B: Global vs. local demeaning treatment. Panel C: Pre-COVID sample restriction (1959-2019). Panel D: Outlier adjustment using interquartile range methodology. Panel E-F: Alternative forecast horizons (8 vs. 12 quarters). (b) Stacked bars show the breakdown in to aggregate factor shares (dark blue), total connectedness across sectors (medium blue) and purely idiosyncratic shares (gray) that sum to 100%.

Monetary Policy Implications. – The results challenge conventional approaches to measuring core inflation that exclude volatile sectors such as food and energy. The analysis shows that food is the strongest net transmitter of spillovers, while gasoline continues to exert persistent transmission effects even over 16-quarter horizons. These sectors' influence extends well beyond their direct price contributions, propagating through the network and amplifying aggregate inflation in ways that conventional core measures fail to capture.

The identification of food services, furnishings, and personal care as key transmission hubs implies that policymakers should monitor these sectors not only for their direct impact on inflation but also for their capacity to generate broader price pressures. Moreover, monetary policy transmission may itself operate through these sectoral linkages, as sectors with high spillover potential can amplify or dampen policy effects across the economy.

The prominence of cross-sectoral spillovers also suggests that inflation forecasting and policy calibration should explicitly incorporate network dynamics rather than relying solely on aggregate relationships. Standard models that relate aggregate inflation to measures of aggregate slack risk overlooking important propagation channels that operate through inter-sectoral connections.

Structural Modeling Implications. — The findings also carry implications for structural multi-sector models. Many current approaches are calibrated using empirical factor model specifications that, as shown here, systematically understate cross-sectoral propagation—by roughly half. Refining empirical specifications to capture these spillovers more accurately can meaningfully alter the conclusions drawn from structural models.

Furthermore, the evidence points to the presence of frictions that interact with bidirectional input—output linkages, indicating the need to move beyond purely mechanical, forward-propagation assumptions. Incorporating richer propagation mechanisms would allow structural models to more accurately assess the aggregate consequences of sectoral policies and shocks.

7 Conclusion

This paper quantifies cross-sectoral spillovers in inflation dynamics using a factor-adjusted network approach that jointly models common factors and sectoral propagation dynamics. The baseline specification avoids systematic biases affecting conventional methods: a pure VAR without factors overestimates spillovers by conflating aggregate comovements with direct transmission, while factor-model approaches underestimate spillovers by assuming independent idiosyncratic components.

Three main findings emerge from the analysis. First, cross-sectoral spillovers are substantial, accounting for 39.9% of total price variation—nearly twice the contribution of aggregate factors (17%)—establishing spillovers as a central driver of inflation dynamics. Second, the baseline model consistently identifies food, furnishings, and service sectors as the leading net transmitters and highlights gasoline as a persistently relevant transmitter over 8- to 16-quarter horizons, in contrast to conventional models that systematically mischaracterize sectoral roles. Third, Monte Carlo validation demonstrates that the baseline specification outperforms conventional restricted models across multiple exercises, confirming its ability to capture the joint influence of aggregate and sectoral propagation channels. Taken together, these results establish the presence of strong cross-sectoral spillovers in inflation and demonstrate that their magnitude reflects not only production networks but also sectoral heterogeneities and nominal frictions absent from frictionless models.

The evidence has important implications for policy and research. For policymakers, the results suggest that monetary policy should account for network effects when assessing sectoral shocks, as spillovers amplify the aggregate consequences of sector-specific disturbances well beyond their direct contributions. For researchers, the findings highlight the need for structural modeling frameworks that incorporate both factor-driven and propagation-driven spillovers, since conventional approaches systematically mischaracterize sectoral influences when cross-sectoral dynamics are excluded.

Future research could extend this framework in several directions, including nonlinear propagation mechanisms, semi-structural identification schemes, and time-varying spillover networks. The factor-adjusted network approach developed here provides a foundation for understanding sectoral interconnections while underscoring the quantitative importance of jointly modeling aggregate and sectoral channels in the analysis of inflation dynamics.

Acknowledgements

The author is grateful to Benjamin Wong, Isaac Gross, Alexander Haas, Laura Puzzello, Qingyuan Du and participants of the MIG meeting at Monash University, Workshop of Australasian Macroeconomic Society (WAMS), OzMac Workshop and European Winter Meeting of Econometric Society for their helpful comments. The views expressed are those of the author and do not necessarily represent the official views of the Bank of Korea. The assistance of AI was employed for grammar refinement; all substantive intellectual contributions remain the responsibility of the author.

Supplementary Materials and Data Availability

An online appendix, submitted as supplementary material, accompanies this manuscript and provides additional figures, robustness checks, and methodological details. Replication code is available from the author upon request.

References

- Acemoglu, D., Carvalho, V. M., Ozdaglar, A., and Tahbaz-Salehi, A. (2012). The network origins of aggregate fluctuations. *Econometrica*, 80(5):1977–2016.
- Acemoglu, D., Carvalho, V. M., Ozdaglar, A., and Tahbaz-Salehi, A. (2017). Production networks and the propagation of economic shocks. *American Economic Review*, 107(11):3253–3288.
- Ahn, J. H. and Luciani, M. (2025). Common and idiosyncratic inflation. *Journal of Applied Econometrics*, n/a(n/a).
- Baqaee, D. R. and Farhi, E. (2019). The macroeconomic impact of microeconomic shocks: Beyond Hulten's theorem. *Econometrica*, 87(4):1155–1203.
- Baqaee, D. R. and Farhi, E. (2020). Productivity and misallocation in general equilibrium. *The Quarterly Journal of Economics*, 135(1):105–163.
- Barigozzi, M. and Brownlees, C. (2019). NETS: Network estimation for time series. *Journal of Applied Econometrics*, 34(3):347–364.
- Barigozzi, M., Cho, H., and Owens, D. (2024). FNETS: Factor-adjusted network estimation and forecasting for high-dimensional time series. *Journal of Business & Economic Statistics*, 42(3):890–902.
- Bernanke, B., Boivin, J., and Eliasz, P. (2005). Measuring the effects of monetary policy: A factor-augmented vector autoregressive (FAVAR) approach. *The Quarterly Journal of Economics*, 120(1):387–422.
- Boivin, J., Giannoni, M. P., and Mihov, I. (2009). Sticky prices and monetary policy: Evidence from disaggregated us data. *The American Economic Review*, 99(1):350–384.
- Carvalho, C., Lee, J. W., and Park, W. Y. (2021). Sectoral price facts in a sticky-price model. *American Economic Journal: Macroeconomics*, 13(1):216–56.
- Carvalho, V. and Gabaix, X. (2013). The great diversification and its undoing. *American Economic Review*, 103(5):1697–1727.
- Das, S., Magistretti, G., Pugacheva, E., and Wingender, P. (2022). Sectoral spillovers across space and time. *Journal of Macroeconomics*, 72(C):None.

- De Graeve, F. and Schneider, J. D. (2023). Identifying sectoral shocks and their role in business cycles. *Journal of Monetary Economics*, 140(C):124–141.
- Demirer, M., Diebold, F. X., Liu, L., and Yilmaz, K. (2018). Estimating global bank network connectedness. *Journal of Applied Econometrics*, 33(1):1–15.
- Diebold, F. and Yilmaz, K. (2014). On the network topology of variance decompositions: Measuring the connectedness of financial firms. *Journal of Econometrics*, 182(1):119–134.
- Diebold, F. X. and Yilmaz, K. (2009). Measuring financial asset return and volatility spillovers, with application to global equity markets. *Economic Journal*, 119(534):158–171.
- Diebold, F. X. and Yilmaz, K. (2012). Better to give than to receive: Predictive directional measurement of volatility spillovers. *International Journal of Forecasting*, 28(1):57–66.
- Diebold, F. X. and Yilmaz, K. (2023). On the past, present, and future of the diebold–yilmaz approach to dynamic network connectedness. *Journal of Econometrics*, 234:115–120. Jubilee Issue Celebrating our Fiftieth Anniversary: 1973–2023.
- Fernald, J. G. (2012). A quarterly, utilization-adjusted series on total factor productivity. Working Paper 2012-19, Federal Reserve Bank of San Francisco.
- Foerster, A. T., Sarte, P.-D. G., and Watson, M. W. (2011). Sectoral versus aggregate shocks: A structural factor analysis of industrial production. *Journal of Political Economy*, 119(1):1–38.
- Furkan, A., Miranda-Pinto, J., Morley, J., Panchenko, V., and Rose, C. (2025). Factor augmented network vector autoregression (FANVAR). Unpublished working paper, distributed in slides.
- Gabaix, X. (2011). The granular origins of aggregate fluctuations. Econometrica, 79(3):733-772.
- Ghassibe, M. (2021). Monetary policy and production networks: an empirical investigation. *Journal of Monetary Economics*, 119:21–39.
- Giannone, D., Lenza, M., and Primiceri, G. E. (2021). Economic predictions with big data: The illusion of sparsity. *Econometrica*, 89(5):2409–2437.
- Horvath, M. (1998). Cyclicality and sectoral linkages: Aggregate fluctuations from independent sectoral shocks. *European Economic Review*, 42(2):311–321.
- Horvath, M. (2000). Sectoral shocks and aggregate fluctuations. Journal of Monetary Economics, 45(1):69-106.
- Hulten, C. R. (1978). Growth accounting with intermediate inputs. The Review of Economic Studies, 45(3):511–518.
- Kilian, L. (2009). Not all oil price shocks are alike: Disentangling demand and supply shocks in the crude oil market. *American Economic Review*, 99(3):1053–69.
- Kilian, L. (2019). Measuring global real economic activity: Do recent critiques hold up to scrutiny? *Economics Letters*, 178:106–110.
- Kohavi, R. (1995). A study of cross-validation and bootstrap for accuracy estimation and model selection. In *Proceedings* of the 14th international joint conference on artificial intelligence (IJCAI), pages 1137–1145. Morgan Kaufmann Publishers Inc.
- Koop, G., Pesaran, M. H., and Potter, S. M. (1996). Impulse response analysis in nonlinear multivariate models. *Journal of Econometrics*, 74(1):119–147.
- Li, N. and Martin, V. L. (2019). Real sectoral spillovers: A dynamic factor analysis of the Great Recession. *Journal of Monetary Economics*, 107:77–95.

- Long, J. B. and Plosser, C. I. (1983). Real business cycles. Journal of Political Economy, 91(1):39-69.
- Luo, S. and Villar, D. (2023). Propagation of shocks in an input-output economy: Evidence from disaggregated prices. *Journal of Monetary Economics*, 137:26–46.
- Meinshausen, N. and Bühlmann, P. (2010). Stability selection. *Journal of the Royal Statistical Society: Series B* (*Statistical Methodology*), 72(4):417–473.
- Miao, K., Phillips, P. C., and Su, L. (2023). High-dimensional VARs with common factors. *Journal of Econometrics*, 233(1):155–183.
- Mlikota, M. (2025). Cross-sectional dynamics under network structure: Theory and macroeconomic applications.
- Moon, H. R. and Weidner, M. (2023). Nuclear norm regularized estimation of panel regression models. arXiv preprint.
- Nakamura, E. and Steinsson, J. (2008). Five facts about prices: A reevaluation of menu cost models. *The Quarterly Journal of Economics*, 123(4):1415–1464.
- Newman, M. (2010). Networks: An Introduction. Oxford University Press.
- Pasten, E., Schoenle, R., and Weber, M. (2020). Monetary policy and sectoral reallocation. *American Economic Review*, 110(1):332–363.
- Pasten, E., Schoenle, R., and Weber, M. (2024). Price rigidity and the propagation of sectoral shocks. *Journal of Monetary Economics*, 119:99–113.
- Pesaran, M. H. and Shin, Y. (1998). Generalized impulse response analysis in linear multivariate models. *Economics Letters*, 58(1):17–29.
- Reis, R. and Watson, M. W. (2010). Relative goods' prices, pure inflation, and the Phillips correlation. *American Economic Journal: Macroeconomics*, 2(3):128–157.
- Rubbo, A. (2023). A structural approach to monetary policy. Review of Economic Studies, 90(1):415-448.
- Schneider, J. D. (2023). The sectoral origins of current inflation. Unpublished manuscript.
- Smets, F., Tielens, J., and Van Hove, J. (2019). Pipeline pressures and sectoral inflation dynamics. *NBB Working Paper Series*, (2019).
- Stock, J. and Watson, M. (2016). Dynamic factor models, factor-augmented vector autoregressions, and structural vector autoregressions in macroeconomics. volume 2, chapter Chapter 8, pages 415–525. Elsevier.
- Tukey, J. W. (1960). A survey of sampling from contaminated distributions.

Online Appendix for Sectoral Spillovers and Inflation Dynamics

August 13, 2025

Yun Young Gwak¹

A Motivating evidence

Sectoral price dynamics underlying aggregate inflation exhibit substantial and persistent heterogeneity. Figure A1 shows that the relationship between aggregate inflation and sectoral price dispersion is not straightforward. During the Great Inflation of the 1970s and the recent post-COVID surge, broad sectoral movements coincided with elevated aggregate inflation, indicating reinforcement across many sectors. By contrast, during the Great Moderation aggregate inflation remained subdued despite considerable dispersion, consistent with sectoral shocks being largely idiosyncratic and offsetting in the aggregate. The conventional view has treated such offsetting as the norm, reducing the incentive to scrutinize sectoral detail. Yet the figure makes clear that this is not always the case: periods of broad-based sectoral alignment can magnify inflationary pressures, highlighting the need to look beneath the aggregate to understand sectoral propagation mechanisms.

This heterogeneity motivates a re-examination of the microeconomic foundations of inflation and the channels through which sectoral shocks propagate. Standard macroeconomic frameworks often abstract from sectoral structure, attributing inflation primarily to aggregate demand and supply shifts or common monetary shocks. The persistent dispersion in sectoral price behavior documented here underscores the importance of sector-specific shocks and their transmission through input—output linkages, demand substitution, and factor market interactions. Recognizing these mechanisms motivates a disaggregated analysis of the sectoral drivers of aggregate inflation and the quantification of spillover effects across prices and quantities.

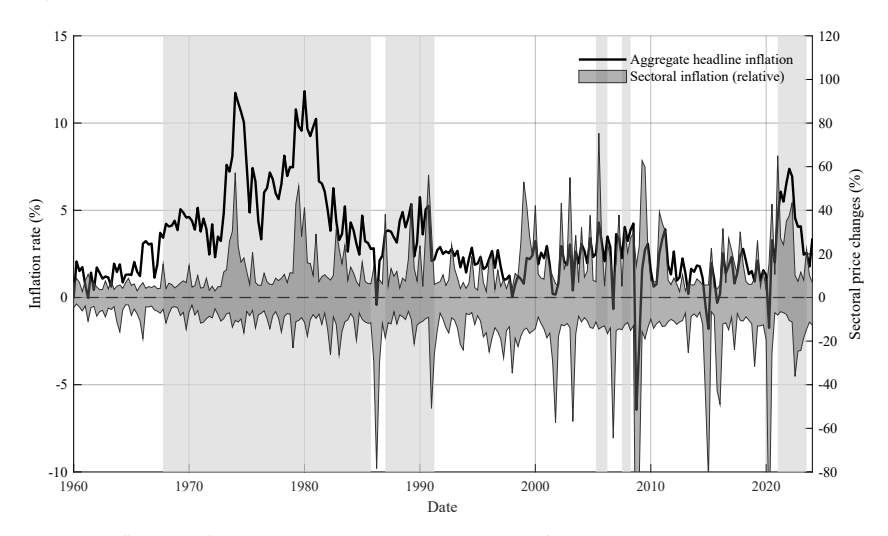


Figure A1: U.S. AGGREGATE INFLATION AND SECTORAL PRICE CHANGES

Note: U.S. aggregate headline inflation (left axis, solid black line) and the range of sectoral price changes relative to aggregate inflation (right axis, shaded gray area), 1960–2024. Shaded regions mark periods when the four-quarter moving average of aggregate inflation exceeds its sample median. Sectoral price changes are annualized quarterly growth rates relative to aggregate inflation, showing the minimum and maximum deviations across 26 PCE sectors. Dispersion widens during inflationary episodes. Data: BEA and BLS, 1960Q1–2024Q2.

¹Correspondence to: Department of Economics, Monash University, 900 Dandenong Road, Caulfield East, Victoria 3145, Australia. E-mail: yunyoung.gwak@monash.edu.

B Data

This section presents time series plots and summary statistics for the Personal Consumption Expenditures (PCE) sectoral price and consumption series obtained from the U.S. Bureau of Economic Analysis, covering the period from 1959:Q1 to 2024:Q2, in Figure B1 and Table B2. Supplementary data are detailed in Table B1.

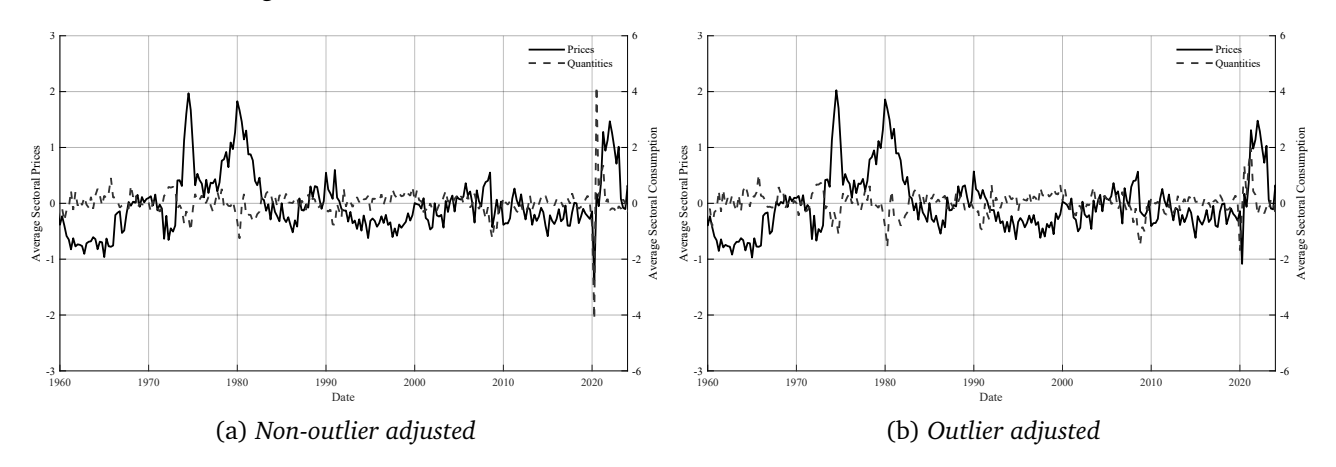


Figure B1: Average movement in Sectoral Price and Consumption

Note: This figure displays average movements in sectoral prices (black line) and sectoral consumption (blue line) for the non-outlier adjusted sample (left) and an outlier-adjusted sample (right).

Table B1: Supplementary Data Description

Variables	Definition	Sample	Source
Unemployment	The deviation of the quarterly moving average of the monthly seasonally adjusted unemployment	1960:Q2-	BLS, CBO
gap	rate (UNRATE) from the quarterly non-cyclical rate of unemployment (NROU).	2024:Q2	(FRED)
Output gap	The deviation of the quarterly seasonally adjusted annual rate of real gross domestic product in	1960:Q2-	BEA,
	billions of chained 2017 dollars (GDPC1) from the quarterly real potential gross domestic product in	2024:Q2	CBO
	billions of chained 2017 dollars (GDPPOT), expresseed as percent changes.		(FRED)
Federal funds	The Federal Funds effective rate is the quarterly moving average of the monthly non-seasonally	1960:Q2-	FRB
rate	adjusted rates (FEDFUNDS).	2024:Q2	(FRED)
Global activity	The index of global real economic activity in industrial commodity markets, proposed by Kilian (2009)	1960:Q2-	FRB of
	and revised in Kilian (2019), as percent deviations from trend.	2024:Q2	Dallas
TFP growth	Business sector total factor productivity growth is defined as quarterly output growth less the contri-	1960:Q2-	Fernald
	butions of capital and labor, measured as percentage changes at an annual rate. The estimates are developed in Fernald (2012) and updated on July 1, 2024.	2024:Q1	(2012)
Adjusted TFP	Utilization-adjusted total factor productivity growth is defined as the growth in total factor productivity	1960:O2-	Fernald
growth	for the business sector, adjusted for the utilization rates of capital and labor. It is measured as the percentage change at an annual rate.	2024:Q1	(2012)
Inflation ex-	Inflation expectation is the quarterly moving average of monthly non-seasonally adjusted median	1978:O1-	Michigan
pectations	expected price changes over the next 12 months, measured in Surveys of Consumers (MICH).	2024:Q2	(FRED)
Sectoral con-	For 26 PCE sectors, share of nominal PCE consumption expenditure out of total nominal PCE con-	-	BEA,
sumption	sumption expenditure, averaged over 1959:Q1-2024:Q2. For 58 BEA industries, consumption shares		PSW(2020
share	in 2002 are sourced from Pasten et al. (2020).		·
Frequency of	For 26 PCE sectors, frequency of price adjustment is sourced from Nakamura and Steinsson (2008).	-	NK(2008)
Price Adjust- ment	For 58 BEA industries, frequency of price adjustment is sourced from Pasten et al. (2020).		PSW(2020
Input-Output	For 58 BEA industries, input output matrix measures how many units of input from row sector i are	2002	BEA,
Matrix	required for output in column sector j as ratios.		PSW(2020
PCE Concor-	The concordance table maps the 58 BEA industries into 26 PCE sectors. The 26 by 58 matrix is	2002	BEA
dance Table	column-wise normalized so that the corresponding values for 58 sectors are distributed across 26 sectors.		

Note: BLS (Bureau of Labor Statistics); CBO (Congressional Budget Office); FRB (Board of Governors of the Federal Reserve System); Series obtaind from FRED are indicated in parantheses.

Table B2: Summary Statistics: Disaggregated PCE Sectoral Price and Consumption Series

Sectors				Prices				Consumption			
Categories	Weight	Infreq.	Duration	Mean	Stdv	ADF	JB	Mean	Stdv	ADF	JB
Durables											
1. New motor vehicle and parts	4.05%	0.52	2.08	1.91	3.64	0.00	0.00	3.36	30.48	0.00	0.00
2. Furnishings and durable household equipment	3.42%	0.48	1.93	1.04	3.52	0.00	0.00	4.25	7.74	0.00	0.00
3. Video, audio equipment and media	1.57%	0.46	1.86	-5.14	5.45	0.00	0.00	12.65	10.19	0.00	0.00
4. Other recreational goods and vehicles	1.07%	0.69	3.23	1.07	4.87	0.00	0.01	5.64	16.88	0.00	0.00
5. Other durable goods	1.54%	0.55	2.23	1.62	4.36	0.00	0.00	4.85	13.38	0.00	0.00
Non-durables											
6. Food and nonalcoholic beverages	9.76%	0.32	1.47	3.30	4.36	0.00	0.00	1.52	4.04	0.00	0.00
7. Alcoholic beverages and food on farms	1.48%	0.49	1.97	2.34	2.95	0.00	0.00	-0.78	10.57	0.00	0.00
8. Garments	4.08%	0.31	1.46	0.94	3.74	0.00	0.00	3.72	10.53	0.00	0.00
9. Other clothing materials and footwear	0.97%	0.41	1.69	1.74	3.46	0.00	0.00	3.07	10.74	0.00	0.00
10. Gasoline and other energy goods	3.57%	0.00	1.00	4.13	26.97	0.00	0.00	1.12	9.29	0.00	0.00
11. Pharmaceutical and other medical products	1.97%	0.61	2.58	3.19	3.33	0.00	0.50	5.07	5.96	0.00	0.00
12. Recreational items, periodicals and stationery	2.13%	0.76	4.09	1.96	3.90	0.00	0.00	2.91	11.79	0.00	0.00
13. Household supplies and personal care products	2.46%	0.58	2.39	2.74	4.92	0.00	0.00	1.23	3.47	0.00	0.00
14. Tobacco	1.19%	0.31	1.44	0.89	2.57	0.00	0.00	3.82	7.45	0.00	0.00
Services											
15. Housing	14.82%	0.72	3.59	3.71	2.16	0.00	0.00	2.81	1.82	0.00	0.00
16. Household utilities	3.04%	0.21	1.27	4.02	5.63	0.00	0.00	2.05	10.91	0.00	0.21
17. Health care	12.08%	0.86	7.01	4.71	3.10	0.00	0.00	3.58	6.70	0.00	0.00
18. Motor vehicle services	2.10%	0.50	2.01	3.80	3.04	0.00	0.00	2.60	7.12	0.00	0.00
19. Public transportation	1.08%	0.18	1.22	3.34	8.48	0.00	0.00	3.59	39.81	0.00	0.00
20. Recreational services	3.08%	0.73	3.66	3.54	1.89	0.00	0.00	3.96	12.78	0.00	0.00
21. Food services	5.75%	0.85	6.67	4.09	2.45	0.00	0.00	2.38	11.52	0.00	0.00
22. Accommodations	0.71%	0.25	1.33	4.06	6.12	0.00	0.00	4.09	36.03	0.00	0.00
23. Financial services and insurance	6.30%	0.78	4.55	3.97	5.49	0.00	0.00	3.39	6.04	0.00	0.00
24. Communication	1.88%	0.31	1.46	0.81	4.04	0.00	0.00	5.62	4.82	0.00	0.21
25. Education services	1.64%	0.82	5.60	5.39	4.15	0.00	0.00	2.01	4.77	0.00	0.00
26. Other services	4.64%	0.86	7.25	4.21	2.37	0.00	0.00	1.41	5.98	0.00	0.00
Total	96.38%		·		·			·			

Note: 1) The 26 sectors include 48 fourth-tier household PCE consumption expenditure categories, excluding used motor vehicles and recreational books, aggregated by similar degrees of nominal rigidity, following Carvalho et al. (2021). 2) The weights (%) are computed from nominal consumption expenditure indices, averaged from 1959:Q1 to 2024:Q2. 3) Infrequency of price adjustment and duration of price spells (in quarters) are sourced from Nakamura and Steinsson (2008). All price and consumption series were transformed appropriately for analysis in VARs and factor estimations by taking the first difference of logs and standardized by local demeaning and variance scaling. 4) Mean and standard deviations are for the un-standardized series. 5) The ADF refers to the augmented Dickey-Fuller unit root test p-values, while JB denotes the Jarque-Bera normality test p-values.

C Supplementary Tables

C.1 Factor Selection

Conceptually, aggregate and sectoral shocks are differentiated by the density of loadings and the scope of their impact. Aggregate shocks affect all sectors simultaneously, though their influence varies across sectors, resulting in less variation between sectors compared to sectoral shocks. In contrast, sectoral shocks have concentrated effects, leading to greater variation in impact within specific sectors, including the originating sector. This distinction aligns with established literature (e.g., Boivin et al., 2009; De Graeve and Schneider, 2023), which highlights differences in sectoral rankings caused by aggregate versus sectoral shocks.

The identification of aggregate shocks relies on the assumption that the common factors capture only broad economy-wide movements from aggregate sources. However, it is possible that the rapid propagation of large sectoral shocks may be misestimated as a factor. the initial unrestricted estimates revealed strong comovements with oil variables. To ensure the validity of the identification assumption, the factors reported in this paper have been estimated under additional orthogonality constraints, ensuring their independence from oil-sector-specific shocks, as detailed at the end of this section. This approach prevents the absorption of large, sector-specific effects into the aggregate factors. The factors are then carefully selected through a series of statistical tests to confirm that the estimated factors genuinely represent aggregate shocks and adequately characterize aggregate dynamics.

The analysis reveals that three factors are necessary to capture aggregate dynamics in both the baseline model and the DFM. This conclusion is supported by various statistical tests, which detect significant reductions in singular values or eigenvalues when additional factors beyond three are considered. Furthermore, the substantial share of variation explained by these three factors, along with their strong correlations with standard aggregate variables representing supply-side, demand-side, and financial factors, reinforce their relevance.

First, Table C1 in the appendix summarizes the factor test results, indicating the combined dataset including both price and consumption, requires up to two factors to explain significant comovements, while the DFM requires up to three factors. Separate tests applied to price and consumption series show that consumption has two factors, while price has one principal factor. Given concerns that the more volatile consumption series in the dataset might dominate factor estimation, potentially causing the two factors in the combined dataset to explain only consumption, up to three factors were examined for both prices and consumption. The analysis confirms the need for three factors, as the third factor is found to be more significant for prices. This is evidenced by its strong explanatory role in Table C2 and the statistical significance of its loadings on prices in Table C3.²

To ensure that each of the three factors represents aggregate dynamics, I examine their explanatory role by series and by period, as well as their correlation with aggregate covariates.³ To begin with, the first factor reflects the excess volatility in mostly consumption series during extreme episodes, reflecting mostly demand-driven shocks, as evidenced by its high correlation with consumption movements during the COVID-19 period. It accounts for 50% of the variance in consumption and 19% in prices in the post-COVID period (Table C2), and has a positive ratio of factor loadings on prices over those on consumption (Table C3), suggesting a strong demand-side influence. The factor's loadings are highest for sectors like 'Accommodations' and 'Public Transport,' which experienced significant disruptions during the pandemic. However, this factor is less significant in pre-COVID and outlier-adjusted datasets, emphasizing its COVID-specific nature.⁴

Meanwhile, the second and third factors appear to broadly capture real and nominal aggregate shocks, respectively.

²For robustness, up to four factors were examined and the fourth factor was found to be insignificant. The factor loadings and their significance levels are reported in the Table C4.

³It is important to note that the interpretation of the factors comes with a caveat: this paper does not attempt to identify the structural sources of the aggregate shocks. The primary focus of the paper is on sectoral dynamics, ensuring that an appropriate number of factors controls for the aggregate dynamics.

⁴In the pre-covid sample and the outlier-adjusted sample, one less factor is identified, likely reflecting the exclusion of COVID effects.

The second factor correlates strongly with total factor productivity growth, the unemployment gap, and the global activity index for industrial commodity markets as shown in Table C2. Its effects on prices and consumption are opposite, as reflected by the negative average ratio of factor loadings on prices relative to consumption, indicating a modest supply-side dominance. In contrast, the third factor captures nominal drivers for prices, and is closely associated with the global activity index and changes in the effective federal funds rate. It disproportionately explains prices (11%) more than consumption (5%), highlighting its primary influence on prices. The highest loadings of the third factor are observed in sectors like 'Gasoline and Energy Goods' and 'Finance' (Table C3).

A final note before concluding this section concerns the transformation of factors to be orthogonal to large sectoral shocks from the oil sector. As briefly mentioned in the beginning of the section, initial estimations showed high correlations between the third factor and real oil prices, indicating the influence of oil-market-specific shocks. Thus, to isolate aggregate shocks from sector-specific oil shocks, factors were orthogonalized using projection matrices for the oil supply and demand shocks. Orthogonalization reduces the correlation of the third factor with real oil prices from over 50% to 30%, attributing the remaining correlation to aggregate demand shocks tied to global activity indices. This supports interpreting the third factor as a nominal aggregate shock, independent of sectoral influences.

All in all, the factor estimation results outlined in this section support the presence of three factors in the baseline dataset, capturing the key aggregate influences in sectoral price and consumption data. This low-rank factor structure is consistent with prior research, which identifies that relatively few factors are sufficient to capture aggregate dynamics. For example, Bernanke et al. (2005) identified just one unobserved factor for real activity, orthogonal to one observed factor identified from the federal funds rate, while Boivin et al. (2009) included five unobserved factors alongside the federal funds rate in a large panel dataset. Similarly, Carvalho et al. (2021) used sectoral price data to identify two unobserved factors at the quarterly frequency, although they excluded consumption series and limited their sample to the Great Moderation period, potentially reducing the number of factors.

(3) Pre-COVID, un-adj. (1) Full, un-adj. (2) Full, adj. Total Prices Consumption Total Prices Consumption Total Prices Consumption A. VAR with Common Factors Bai-Ng ICp1 Bai-Ng ICp2 Bai-Ng ICp3 Ahn-Hornstein Eigenvalue Ratio B. FAVAR Bai-Ng ICp1 Bai-Ng ICp2 Bai-Ng ICp3 Ahn-Hornstein Eigenvalue Ratio

Table C1: FACTOR TEST STATISTICS

Note: Panel A reports factor tests on residuals $(Y - X\beta)$; Panel B on raw data (Y). ICp1-3 follow Bai & Ng (2002); Eigenvalue Ratio from Ahn & Horenstein (2013). Columns (1)–(3) reflect: full sample, outlier-adjusted, and pre-COVID data. 'Total' combines all data.

⁵For the oil shock identification, an extension of Kilian (2009)'s structural oil supply and demand shocks from 1975 to 2024 has been employed. The orthogonalization proceeds as follows: Suppose F is the matrix one wishes to orthogonalize and B is the matrix whose influence one wishes to project out from F, then the projection matrix in the Gram-Schmidt process that projects any vector onto the space spanned by columns of B is constructed as $P_B = B(B^TB)^{-1}B^T$. Then the orthogonalized F is calculated as $F^{\perp} = F - P_B F$ where $P_B F$ is the component of F that lies in the space of B.

Table C2: FACTOR VARIANCE SHARES AND CORRELATION WITH AGGREGATES

	(1) Full, un-adj.			((2) Full, adj		(3) Pre-covid, un-adj.			
	Factor 1	Factor 2	Factor 3	Factor 1	Factor 2	Factor 3	Factor 1	Factor 2	Factor 3	
A. Full										
Prices	0.03	0.07	0.10	0.02	0.12	0.04	-	-	-	
Consumption	0.24	0.08	0.03	0.17	0.06	0.05	-	-	-	
B. Pre-Covid										
Prices	0.01	0.07	0.11	0.01	0.10	0.04	0.04	0.14	0.04	
Consumption	0.07	0.11	0.05	0.15	0.05	0.04	0.16	0.04	0.04	
C. Post-Covid										
Prices	0.20	0.07	0.03	0.03	0.25	0.07	-	-	-	
Consumption	0.54	0.03	0.01	0.23	0.09	0.06	-	-	-	
D. Aggregates										
ΔUnemployment Gap	-0.66***	0.09	0.04	-0.06	0.10	0.26***	-0.13*	0.20***	-0.21***	
Unemployment Gap	-0.10	0.17**	-0.08	-0.16**	-0.03	-0.00	0.10	-0.04	-0.00	
Δ Output Gap	0.62***	0.09	-0.12*	-0.18***	-0.13**	-0.21***	0.31***	-0.18***	0.16**	
Output Gap	0.11*	-0.13*	-0.01	0.11	-0.03	-0.05	-0.08	-0.05	0.00	
ΔEffective Federal funds Rate	0.03	0.11*	-0.14**	-0.07	0.01	-0.14**	0.08	-0.13*	0.18**	
Effective Fed funds Rate	0.05	0.01	-0.05	-0.02	0.01	-0.06	0.08	-0.02	-0.06	
ΔGlobal activity index (Kilian)	0.17**	0.06	-0.12*	-0.21***	-0.12*	-0.02	0.10	-0.20***	-0.00	
Global activity index (Kilian)	0.13*	-0.17**	-0.23***	-0.00	-0.26***	-0.12*	-0.09	-0.26***	-0.09	
Total Factor Productivity (TFP) Growth	0.39***	0.24***	-0.04	-0.25***	-0.02	-0.12*	0.40***	-0.07	0.12*	

Note: Panels A to C present the factor variance shares. Panel D displays Pearson's correlation test statistics between selected aggregate covariates and the factors from 1968 Q1. Δ denotes differenced variables representing changes from the preceding period. For the correlation statistics, significance levels of 1%, 5%, and 10% are indicated by ***, **, and *.

Table C3: RATIO AND SIGNIFICANCE OF FACTOR LOADINGS

	(1	l) Full, un-a	dj.		(2) Full, adj		(3) Pre-covid, un-adj.			
	Factor 1	Factor 2	Factor 3	Factor 1	Factor 2	Factor 3	Factor 1	Factor 2	Factor 3	
Panel A. Loadings										
Prices (P)	0.10	-0.11**	-0.13**	0.04	-0.15***	-0.07	-0.07	-0.13**	0.06	
Consump. (Q)	0.38***	0.13	0.03	-0.31***	0.02	0.01	0.28***	0.02	0.05	
Avg. Ratio (P/Q)	0.25	-0.91	-4.13	-0.11	-9.93	-5.13	-0.26	-6.81	1.27	
Panel B. Top 5 Sectors										
1st	22 (1.32)	4 (0.99)	10 (0.71)	22 (1.32)	4 (0.99)	10 (0.71)	22 (1.32)	4 (0.99)	10 (0.71)	
2nd	8 (1.12)	12 (0.74)	25 (0.66)	8 (1.12)	12 (0.74)	25 (0.66)	8 (1.12)	12 (0.74)	25 (0.66)	
3rd	9 (1.05)	1 (0.61)	23 (0.62)	9 (1.05)	1 (0.61)	23 (0.62)	9 (1.05)	1 (0.61)	23 (0.62)	
4th	19 (1.04)	2 (0.58)	6 (0.59)	19 (1.04)	2 (0.58)	6 (0.59)	19 (1.04)	2 (0.58)	6 (0.59)	
5th	10 (1.00)	13 (0.57)	16 (0.54)	10 (1.00)	13 (0.57)	16 (0.54)	10 (1.00)	13 (0.57)	16 (0.54)	

Note: Panel A displays the average factor loadings on prices and consumption, weighted by the absolute size of the loadings. Significance levels of 1%, 5%, and 10% are indicated by ***, **, and *, respectively. Panel B lists the most influenced sectors, with the sum of absolute factor loadings on both prices and consumption shown in parentheses.

Table C4: RATIO AND SIGNIFICANCE OF LOADINGS WITH FOURTH FACTOR

	Avg Factor 1 Loadings	Avg Factor 2 Loadings	Avg Factor 3 Loadings	Avg Factor 4 Loadings
Prices (P)	0.10	-0.11**	-0.13**	-0.00
Consump (Q)	0.38***	0.13	0.03	0.02
Avg. Ratio (P/Q)	0.26	-0.90	-4.73	-0.02

Note: This table reports results with a fourth factor added. Average factor loadings on prices and consumption are weighted by absolute size. Significance at 1%, 5%, and 10% is denoted by ***, **, and *, respectively.

C.2 Variance Decomposition

Table C5: Variance Decomposition and Diebold-Yilmaz Connectedness by Sector

No.	Sector	Variance Decomposition					Diebold-Yilmaz Connectedness									
		BA	ASE	FAV	/AR	PV	PVAR		BASE		FAVAR			PVAR		
		Agg	Sect	Agg	Sect	Agg	Sect	То	From	Net	То	From	Net	То	From	Net
1	new vehicles	0.099	0.901	0.402	0.598	0.000	1.000	61.91	45.17	16.75	17.01	19.15	-2.14	61.19	54.39	6.80
2	furnishings	0.127	0.873	0.536	0.464	0.000	1.000	86.30	49.81	36.48	25.89	15.10	10.80	90.94	64.09	26.85
3	media	0.092	0.908	0.298	0.702	0.000	1.000	37.47	34.24	3.23	17.21	12.79	4.42	42.89	44.68	-1.80
4	other recreation	0.205	0.795	0.292	0.708	0.000	1.000	48.40	37.18	11.23	21.05	21.27	-0.22	22.82	36.95	-14.13
5	other durable	0.200	0.800	0.382	0.618	0.000	1.000	14.80	35.58	-20.78	12.62	12.09	0.52	59.94	53.38	6.55
6	food	0.201	0.799	0.408	0.592	0.000	1.000	85.38	34.31	51.08	24.62	16.59	8.03	115.00	45.94	69.06
7	alcohol	0.065	0.935	0.208	0.792	0.000	1.000	34.29	38.49	-4.20	14.33	21.36	-7.02	24.59	45.60	-21.01
8	garments	0.305	0.695	0.379	0.621	0.000	1.000	20.62	26.01	-5.39	20.67	15.62	5.05	66.76	67.09	-0.33
9	footwear	0.267	0.733	0.397	0.603	0.000	1.000	21.02	27.36	-6.34	19.82	19.26	0.57	76.40	68.04	8.36
10	gasoline	0.279	0.721	0.158	0.842	0.000	1.000	33.13	23.23	9.90	36.97	32.59	4.38	91.43	56.02	35.41
11	medical	0.094	0.906	0.258	0.742	0.000	1.000	19.84	51.28	-31.45	28.10	25.07	3.02	19.87	64.57	-44.71
12	stationery	0.178	0.822	0.329	0.671	0.000	1.000	30.62	37.91	-7.29	8.67	16.41	-7.73	16.75	44.84	-28.10
13	personal care	0.194	0.806	0.590	0.410	0.000	1.000	78.06	55.91	22.16	29.77	14.99	14.78	67.32	74.28	-6.96
14	tobacco	0.108	0.892	0.059	0.941	0.000	1.000	24.53	24.99	-0.46	9.21	21.83	-12.62	9.44	27.40	-17.96
15	housing	0.087	0.913	0.389	0.611	0.000	1.000	17.21	61.41	-44.20	35.75	19.96	15.79	33.29	74.41	-41.12
16	utilities	0.128	0.872	0.420	0.580	0.000	1.000	26.56	41.07	-14.51	11.29	24.08	-12.79	30.10	63.01	-32.91
17	health care	0.121	0.879	0.476	0.524	0.000	1.000	45.82	51.33	-5.51	12.85	22.08	-9.23	78.36	66.73	11.63
18	vehicle service	0.149	0.851	0.675	0.325	0.000	1.000	42.61	59.29	-16.68	25.43	13.35	12.08	66.92	78.73	-11.81
19	public transport	0.218	0.782	0.187	0.813	0.000	1.000	18.16	25.30	-7.14	20.39	29.49	-9.10	61.55	59.89	1.66
20	recreational service	0.161	0.839	0.518	0.482	0.000	1.000	21.79	52.33	-30.54	18.67	18.16	0.51	73.87	68.13	5.74
21	food service	0.139	0.861	0.672	0.328	0.000	1.000	90.60	59.70	30.90	16.24	19.41	-3.16	133.19	74.84	58.35
22	accommodations	0.314	0.686	0.416	0.584	0.000	1.000	33.57	30.73	2.84	22.09	21.72	0.37	76.47	69.98	6.49
23	finance	0.275	0.725	0.146	0.854	0.000	1.000	22.77	23.61	-0.84	17.77	25.09	-7.32	24.09	47.40	-23.30
24	communication	0.121	0.879	0.052	0.948	0.000	1.000	31.85	28.58	3.27	10.16	17.41	-7.25	15.93	32.55	-16.62
25	education	0.154	0.846	0.093	0.907	0.000	1.000	15.48	28.20	-12.72	12.58	18.29	-5.72	31.62	26.61	5.01
26	other service	0.106	0.894	0.607	0.393	0.000	1.000	75.32	55.10	20.22	16.39	12.41	3.97	89.23	70.39	18.85

Note: This table presents variance decomposition and Diebold-Yilmaz connectedness measures for individual sectors. The variance decomposition columns show the proportion of forecast error variance explained by aggregate vs. sectoral shocks under three model specifications: BASE (baseline VAR), FAVAR (Factor-Augmented VAR), and PVAR (Panel VAR). The Diebold-Yilmaz connectedness columns report directional connectedness measures: "To" indicates spillovers transmitted from each sector to others, "From" indicates spillovers received from others, and "Net" is the difference (To - From), representing net spillover contribution. Positive net values indicate net transmitters of shocks, while negative values indicate net receivers. All connectedness measures are expressed as percentages.

C.3 Dyadic Regression

Table C6: Dyadic Regression with Two-Way Fixed Effects

	(1)	(2)	(3)	(4)	(5)	(6)	(7)
IO	2.027**	3.020***	1.950**	2.467***	2.449***	3.379***	1.922**
	(0.880)	(0.838)	(0.895)	(0.848)	(0.888)	(0.861)	(0.936)
ShareOut	3.654***	3.304***	4.918***	3.465***	3.435***	3.146***	5.150***
	(0.790)	(0.674)	(1.133)	(0.780)	(0.897)	(0.715)	(0.991)
$IO \times Size_i$		-1.676***	-1.632***			-1.613***	-1.221*
		(0.504)	(0.574)			(0.504)	(0.650)
IO x Size _j		0.560	1.015*			0.550	1.409*
		(0.664)	(0.604)			(0.669)	(0.795)
ShareOut x Size _i			1.274*				0.520
			(0.671)				(0.972)
ShareOut x Size _j			-2.180***				-2.423***
			(0.831)				(0.702)
IO x Rigidity _i				1.101	0.955	0.990	0.481
				(0.705)	(0.651)	(0.874)	(0.699)
IO x Rigidity _j				-0.744	-0.976	-0.670	-1.268
				(0.631)	(0.623)	(0.821)	(0.896)
ShareOut x Rigidity $_i$					-0.002		0.942
					(0.721)		(0.694)
ShareOut x Rigidity _j					0.834		0.929
					(0.704)		(0.872)
Observations	676	676	676	676	676	676	676
Sender Fixed Effects (FE)	Yes	Yes	Yes	Yes	Yes	Yes	Yes
Receiver Fixed Effects (FE)	Yes	Yes	Yes	Yes	Yes	Yes	Yes
R-squared (within)	0.316	0.341	0.372	0.326	0.331	0.348	0.393
R-squared (adj.)	0.315	0.338	0.367	0.323	0.326	0.343	0.385
Akaike Information Criterion (AIC)	4536.4	4515.7	4486.9	4531.0	4529.5	4511.9	4471.7
Bayesian Information Criterion (BIC)	4545.4	4533.8	4514.0	4549.1	4556.6	4539.0	4516.9
Clusters i	26	26	26	26	26	26	26
Clusters j	26	26	26	26	26	26	26

Notes: (a) The dependent variable is the Diebold–Yilmaz pairwise connectedness for sectoral prices, DY_{ij}^p , defined as the share of forecast-error variance of sector j's inflation explained by shocks from sector i (ordered dyads). (b) All models include two-way fixed effects for sender (i) and receiver (j). (c) Reported coefficients are on the first line; heteroskedasticity-robust standard errors clustered by sender are in parentheses. (d) All regressors are standardized, so coefficients reflect the change in connectedness associated with a one–standard-deviation increase. (e) Dyadic regressors: IO_{ij} (direct requirement from i to j) and ShareOut $_{ij}$ (fraction of i's output sold to j). Sector characteristics: $Size_i$, $Size_j$ (sectoral sizes) and $Rigidity_i$, $Rigidity_j$ (price rigidities). Interaction terms allow IO and ShareOut effects to vary with size and rigidity. (f) Columns: (1) IO, ShareOut; (2) add IO \times Size; (3) add ShareOut \times Size; (4) add $IO \times$ Rigidity; (5) add ShareOut \times Rigidity; (6) add $IO \times$ Size and $IO \times$ Rigidity; (7) all interactions. (g) Within- R^2 is reported after absorbing fixed effects. (h) Significance levels: *p < 0.10, **p < 0.05, ***p < 0.01.

D Supplementary Figures

D.1 Variance Decomposition

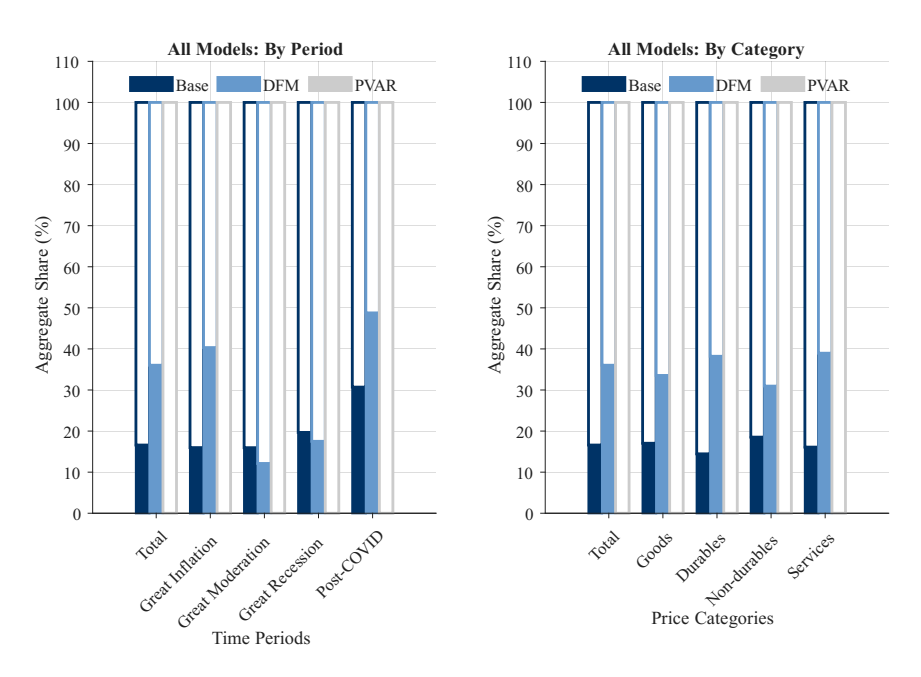


Figure D1: Variance Decomposition Comparison Across All Models

Note: This figure compares variance decomposition across all three model specifications by time periods (left panel) and sectoral categories (right panel). For each period/category, three grouped bars show the baseline model (dark blue), DFM (B=0) (medium blue), and PVAR model (light gray). Each bar represents stacked aggregate shares (filled with model colors) and sectoral shares (white with colored borders) that sum to 100%.

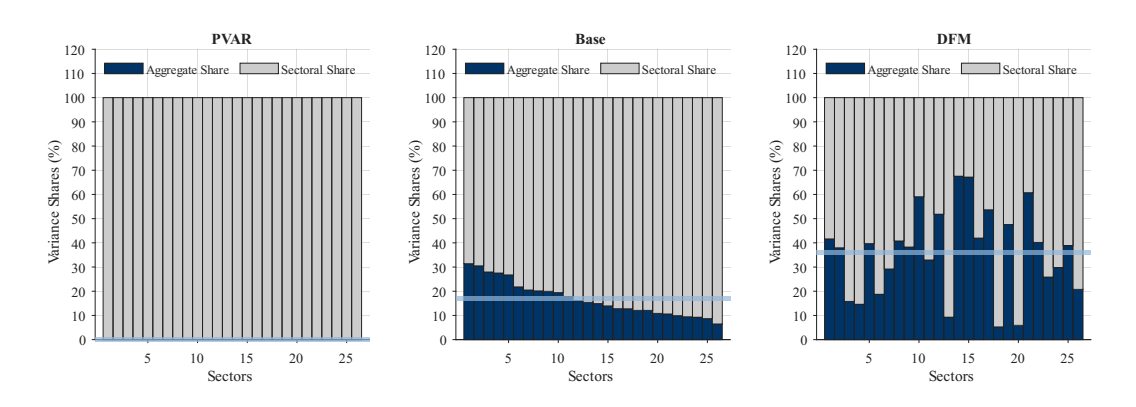


Figure D2: Sectoral Variance Decomposition Across Individual Sectors

Note: This figure compares variance decomposition across all 26 individual sectors for three model specifications. Each panel shows stacked bars with aggregate shares (dark blue) and sectoral shares (light gray) that sum to 100%. Sectors are sorted by baseline model aggregate shares in descending order. The horizontal light blue line indicates the mean aggregate share within each model. Left panel: PVAR model shows zero aggregate shares by construction, with all variation attributed to sectoral dynamics. Center panel: Baseline model reveals substantial heterogeneity across sectors, with aggregate shares ranging from 10% to 45%. Right panel: DFM (B=0) shows higher and more dispersed aggregate shares, reflecting the absorption of spillover effects into factor estimates.

D.2 Monte Carlo Model Evaluation

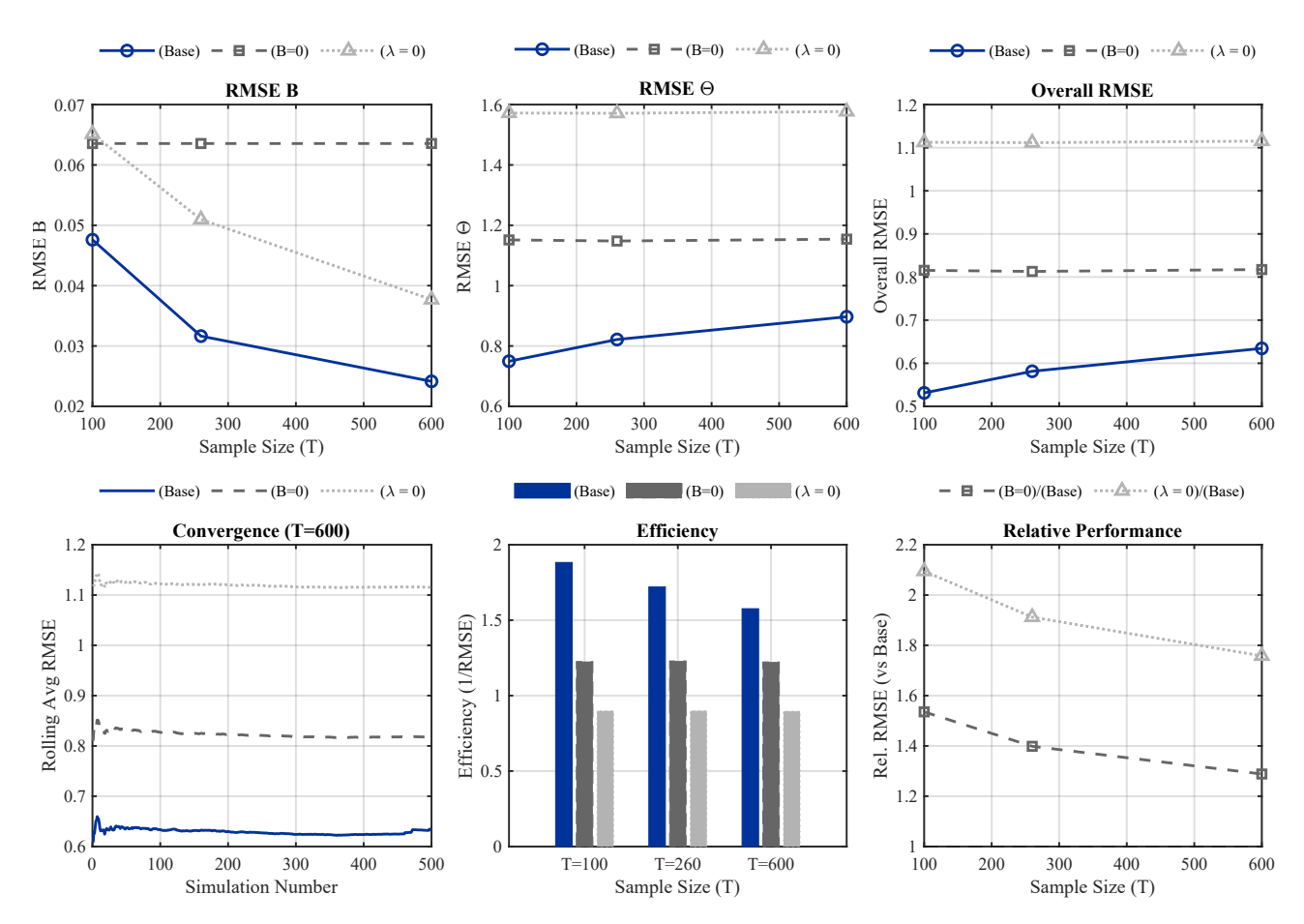


Figure D3: Monte Carlo Validation: Model Performance Across Data Generating Processes Note: This figure shows root mean squared errors (RMSE) for parameter recovery across three model specifications for a data generating processes with both factors (ΛF_t) and cross-sectoral dynamics (B) present. Panel A shows RMSE for transition matrix B recovery. Panel B shows RMSE for common component ΛF recovery. Panel C shows overall prediction RMSE, an average over the previous two. Three sample sizes are considered: T = 100, 260, 600 quarters. Results are based on 500 Monte Carlo replications. The baseline model performs best when both channels exist. This validates that the baseline model accurately captures hybrid dynamics without over-parameterization.